Volume 16
Number 24
21 December 2025
Pages 9249-9646

Food & Function

Linking the chemistry and physics of food with health and nutrition

rsc.li/food-function

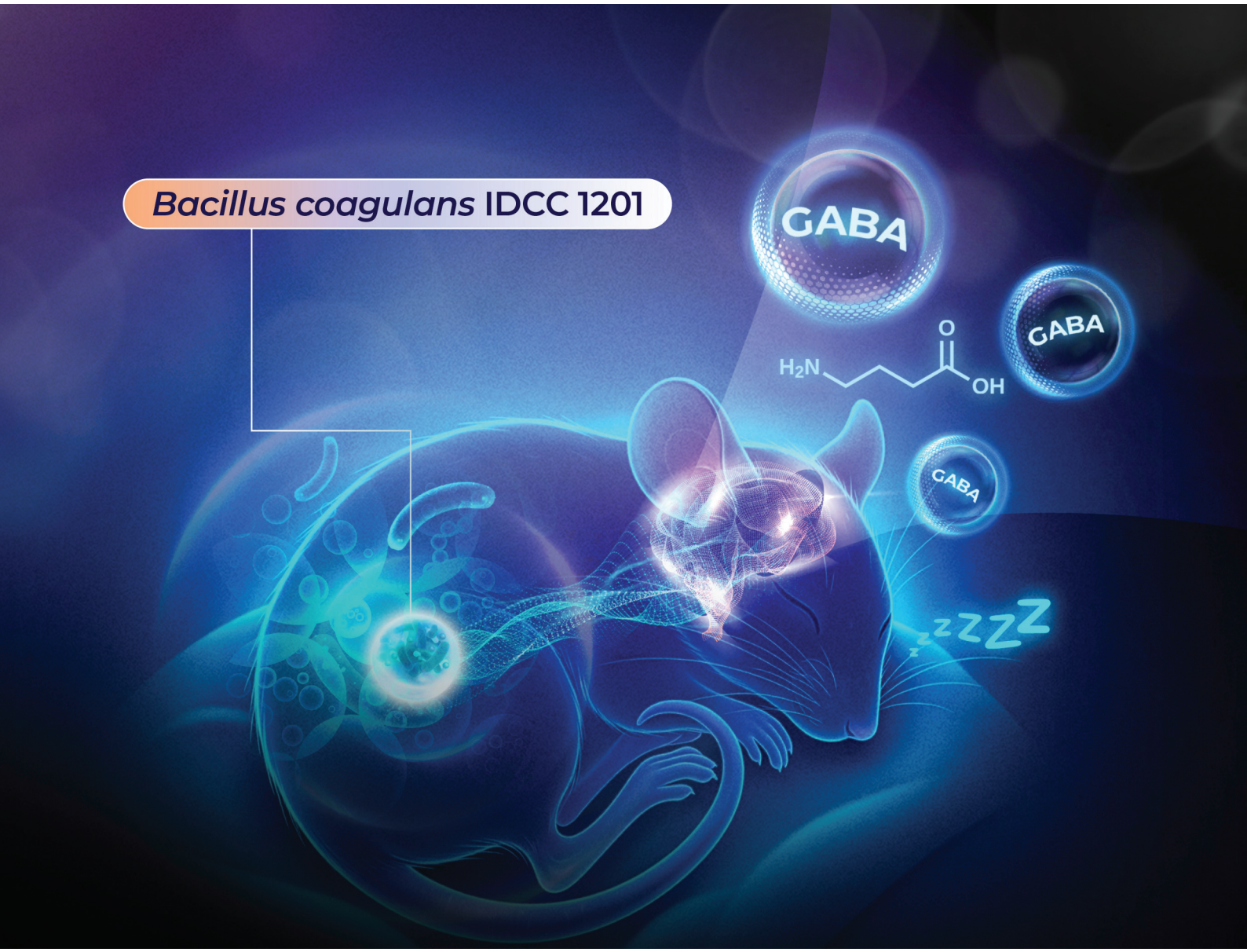

ISSN 2042-650X

ROYAL SOCIETY OF CHEMISTRY

PAPER

Jin Seok Moon *et al.*

Sleep-promoting effects and mechanisms of *Bacillus coagulans* IDCC 1201: evidence from pentobarbital-induced sleep and electroencephalography analysis in mice

Food & Function

ROYAL SOCIETY OF CHEMISTRY

PAPER

View Article Online
View Journal | View Issue

Open Access Article. Published on 19 November 2025. Downloaded on 3/31/2026 6:45:20 AM.
This article is licensed under a Creative Commons Attribution 3.0 Unported Licence.

Check for updates

Cite this: *Food Funct.*, 2025, **16**, 9359

Sleep-promoting effects and mechanisms of *Bacillus coagulans* IDCC 1201: evidence from pentobarbital-induced sleep and electroencephalography analysis in mice

Hayoung Kim, †[a] Won Yeong Bang, [a] Duhyeon Kim, [b] Suengmok Cho, [b] Dong Young Lee, [c] Hyun Min Park, [a] Han Bin Lee, [a] Eun Ju Yun [c] and Jin Seok Moon *[a]

Received 10th July 2025,
Accepted 2nd September 2025

DOI: 10.1039/d5fo02926k

rsc.li/food-function

Recent studies have explored the potential of probiotics to modulate sleep, particularly *via* neurotransmitter pathways. *Bacillus coagulans* IDCC 1201 is a high γ-aminobutyric acid (GABA)-producing strain, second only to *Lactobacillus johnsonii* IDCC 9203. This study investigated the sleep-promoting efficacy of *B. coagulans* IDCC 1201 using a pentobarbital-induced sleep model and electroencephalography (EEG)-based sleep architecture analysis. In the pentobarbital-induced sleep test, *B. coagulans* IDCC 1201 at $\geq 1 \times 10^8$ CFU per day significantly reduced sleep latency and increased sleep duration, showing comparable efficacy to doxepin hydrochloride. Mechanistic studies revealed that the sleep-promoting effects were abolished when it was co-administered with flumazenil, a $GABA_A$ benzodiazepine receptor antagonist, thereby supporting its action *via* the GABAergic system. Furthermore, a long-term EEG study demonstrated that *B. coagulans* IDCC 1201 administration led to a sustained increase in non-rapid eye movement sleep without affecting the stability of wakefulness. In contrast to zolpidem, which showed diminished efficacy over time, *B. coagulans* IDCC 1201 maintained its sleep-promoting effects over three weeks of administration without any signs of tolerance or withdrawal. Delta activity analysis indicated no adverse effects on sleep quality. These findings suggest that *B. coagulans* IDCC 1201 enhances sleep by modulating the GABAergic system and improving sleep architecture, highlighting its potential as a functional ingredient for sleep enhancement without the drawbacks of conventional sleep aids.

Introduction

Probiotics are live microorganisms that confer health benefits when administered adequately, primarily by modulating the gut microbiota and enhancing gastrointestinal function. Traditionally, probiotics have been studied for their effects on gut health and immune function.[1] Emerging research has highlighted their potential influence on the gut–brain axis, a bidirectional communication network that links the gut microbiota to the central nervous system. This connection suggests that gut microbes play a crucial role in neurotransmitter production, stress response, and overall brain function, thereby affecting mental health conditions, such as anxiety, depression, and sleep disorders.[2] One of the key neurotransmitters regulated by the gut microbiota is γ-aminobutyric acid (GABA), the primary inhibitory neurotransmitter in the central nervous system. GABA plays a crucial role in reducing neuronal excitability and promoting relaxation, making it a key factor in sleep initiation and maintenance. Probiotic strains, including *Lactobacillus* and *Bifidobacterium*, reportedly enhance GABA production and modulate GABAergic signaling, leading to anxiolytic and sleep-promoting effects in both animal models and humans.[3] Importantly, *Bacillus coagulans* has also been identified as a GABA-producing probiotic, contributing to its ability to generate beneficial metabolites such as amino acids and vitamins, as well as GABA, which may support its role in sleep promotion and stress reduction.[4] Building on these mechanistic observations, growing evidence links probiotics to improvements in sleep quality *via* the microbiota–gut–brain axis. A recent systematic review and meta-analysis in insomnia reported that probiotics significantly reduced Pittsburgh sleep quality index and Hamilton depression rating scale scores

[a]*Ildong Bioscience, Pyeongtaek-si, Gyeonggi-du, 17957, Republic of Korea. E-mail: moonjs@ildong.com*
[b]*Department of Food Science and Technology, Institute of Food Science, Pukyong National University, Busan 48513, Republic of Korea*
[c]*Department of Biotechnology, The Catholic University of Korea, Bucheon 14662, Republic of Korea*
†The author is first author.

Open Access Article. Published on 19 November 2025. Downloaded on 3/31/2026 6:45:20 AM.
This article is licensed under a Creative Commons Attribution 3.0 Unported Licence.

without increasing adverse events, whereas effects on objective sleep parameters were less consistent, underscoring both promise and remaining gaps. In randomized trials summarized therein, multi-strain formulations reduced Pittsburgh sleep quality index over time and *Lactobacillus plantarum* PS128 improved both sleep quality and mood, consistent with microbiota-mediated modulation of neurotransmitters such as GABA and 5-hydroxytryptamine.[5]

Sleep is a fundamental physiological process for maintaining homeostasis, cognitive function, and overall health.[6] Chronic sleep deprivation or poor sleep quality is associated with various adverse health outcomes, including increased risks of cardiovascular diseases, cognitive impairments, and mental health conditions, such as depression and anxiety.[7] Despite the growing awareness of the importance of sleep, modern lifestyles, including irregular work schedules and excessive screen time, as well as high stress levels, have contributed to an increased prevalence of sleep disorders and insomnia.

Currently, the most widely used pharmacological treatments for sleep disorders are GABA-A receptor agonists, including benzodiazepines (BZDs) (*e.g.*, diazepam and lorazepam) and non-BZD Z-drugs (*e.g.*, zolpidem [ZPD] and eszopiclone). These compounds enhance GABAergic inhibition in the central nervous system, inducing sedative and hypnotic effects.[8] Although these medications are effective at inducing sleep, their long-term use is associated with considerable drawbacks, such as tolerance, dependency, withdrawal (WD) symptoms, cognitive impairments, and next-day drowsiness.[9] Given these limitations, there has been growing interest in exploring natural alternatives, such as herbal extracts, amino acids, and probiotics, that may offer sleep-promoting benefits with fewer side effects.

To effectively assess the sleep-promoting potential of probiotics as natural replacements for pharmacological therapies requires preclinical evaluations using validated sleep models. The pentobarbital-induced sleep test is widely used to evaluate hypnotic activity in rodents, providing quantitative measurements of sleep latency and duration. Additionally, electroencephalography (EEG) allows a detailed examination of sleep architecture, including changes in non-rapid eye movement sleep (NREMS), REMS, and delta wave activity, which are critical markers of sleep quality.[3] Using these methods, we can comprehensively assess whether probiotics exert sleep-promoting effects through GABAergic modulation.

In this study, we aimed to evaluate the sleep-promoting effects of *B. coagulans* IDCC 1201 and elucidate its mechanism of action using pentobarbital sleep tests and EEG-based analysis.

Experimental

Bacterial strains and growth conditions

All probiotics used in this study were obtained from Ildong Bioscience Co., Ltd (Pyeongtaek-si, Gyeonggi-do, Republic of Korea) and stored at −80 °C. All strains, except *Lactococcus lactis* IDCC 2301 and *B. coagulans* IDCC 1201, were anaerobically cultured in De Man, Rogosa, and Sharpe (MRS) medium (BD Difco, Franklin Lakes, NJ, USA) at 37 °C. *B. coagulans* IDCC 1201 was aerobically cultured in MRS medium at 45 °C. *L. lactis* IDCC 2301 was grown aerobically in MRS medium at 37 °C. Detailed information on the culture conditions and probiotic strains is provided in Table 1.

Analysis of GABA production using high-performance liquid chromatography

The probiotic strains were incubated in MRS broth under optimal culture conditions. Cell-free supernatants were obtained *via* centrifugation at 19 500*g* and 4 °C for 10 min, followed by filtration through a 0.45 μm pore-size membrane. *B. coagulans* IDCC 1201 was cultured in MRS broth sup-

Table 1 Probiotic strains used in this study

Strain	Origin	ATCC number	Temperature	Condition
Enterococcus faecium IDCC 2102	Breast-fed infant's feces	BAA-3146	37 °C	Anaerobic
Streptococcus thermophilus IDCC 2201	Homemade yogurt	BAA-3150	37 °C	Anaerobic
Lactococcus lactis IDCC 2301	Homemade cheese	BAA-2834	37 °C	Aerobic
Lactobacillus gasseri IDCC 3101	Breast milk	BAA-2841	37 °C	Anaerobic
Lactobacillus rhamnosus IDCC 3201	Breast-fed infant's feces	BAA-2836	37 °C	Anaerobic
Lactobacillus paracasei IDCC 3401	Breast-fed infant's feces	BAA-2839	37 °C	Anaerobic
Lactobacillus casei IDCC 3451	Breast-fed infant's feces	BAA-2843	37 °C	Anaerobic
Lactobacillus plantarum IDCC 3501	Kimchi	BAA-2838	37 °C	Anaerobic
Lactobacillus salivarius IDCC 3551	Healthy child saliva	BAA-2835	37 °C	Anaerobic
Lactobacillus bulgaricus IDCC 3601	Homemade yogurt	BAA-2844	37 °C	Anaerobic
Lactobacillus reuteri IDCC 3701	Breast milk	BAA-2837	37 °C	Anaerobic
Lactobacillus helveticus IDCC 3801	Breast-fed infant's feces	BAA-2840	37 °C	Anaerobic
Lactobacillus fermentum IDCC 3901	Homemade cheese	BAA-2842	37 °C	Anaerobic
Bifidobacterium longum IDCC 4101	Breast-fed infant's feces	BAA-3145	37 °C	Anaerobic
Bifidobacterium bifidum IDCC 4201	Breast-fed infant's feces	BAA-2850	37 °C	Anaerobic
Bifidobacterium lactis IDCC 4301	Breast-fed infant's feces	BAA-2848	37 °C	Anaerobic
Bifidobacterium breve IDCC 4401	Breast-fed infant's feces	BBA-2849	37 °C	Anaerobic
Lactobacillus johnsonii IDCC 9203	Breast-fed infant's feces	BAA-3147	37 °C	Anaerobic
Bacillus coagulans IDCC 1201	Green malt	BAA-3143	45 °C	Aerobic

 This journal is © The Royal Society of Chemistry 2025

Open Access Article. Published on 19 November 2025. Downloaded on 3/31/2026 6:45:20 AM. This article is licensed under a Creative Commons Attribution 3.0 Unported Licence.

plemented with 0.5% (w/v) monosodium L-glutamate (Food Additive Grade, VEDAN Enterprise Corp Ltd, Dong Nai Province, Vietnam) to evaluate its GABA-producing capability. GABA derivatives were prepared by mixing 300 μL of borate buffer (50 mM, pH 9), 100 μL of methanol, 47 μL of distilled water, 50 μL of the prepared supernatants or GABA standard (Sigma-Aldrich, MO, USA), and 3 μL of diethyl ethoxymethylenemalonate. The mixtures were incubated at 70 °C for 2 h to facilitate the reaction.

GABA was separated using high-performance liquid chromatograph (Agilent 1260, Agilent Technologies, CA, USA) equipped with a C18 column (YMC-Triart, 4.6 × 250 mm, YMC, Kyoto, Japan). The chromatographic conditions are detailed in the SI.

Animal experiments

Sample preparation for animal experiments. The sleep-promoting effects of probiotic strains (*L. johnsonii* IDCC 9203, *B. coagulans* IDCC 1201, and *L. rhamnosus* IDCC 3201) were evaluated using a pentobarbital-induced sleep test. Freeze-dried probiotic strains were provided by Ildong Bioscience (Pyeongtaek-si, Gyeonggi-do, Republic of Korea). All probiotic samples were prepared using a saline solution. Each sample was thoroughly homogenized for 5 min. Before experimentation, all the samples were adequately vortexed using a vortex mixer. The administration dosage for experimental animals was 10 mL kg^{-1}, delivered orally (p.o.) *via* a mouse sonde (gastric tube, ∅ 0.9).

Pentobarbital was purchased from Hanlim Pharm Co. Ltd (Seoul, Korea). Additionally, doxepin hydrochloride (DH), a histamine H1 receptor antagonist, and 2-pyridylethylamine dihydrochloride (2-PD), a histamine H1 receptor agonist, were obtained from Tocris Bioscience (Bristol, UK).[10] For experiments involving the $GABA_A$-BZD receptor, ZPD, an agonist, and flumazenil (FLU), an antagonist, were purchased from the Ministry of Food and Drug Safety (Cheongju, Korea) and Sigma-Aldrich Co., respectively. All drugs were freshly dissolved in sterile saline with 5% Tween 80 immediately before use and administered to mice *via* oral gavage using a sonde needle. DH (30 mg kg^{-1}, p.o.) and ZPD (10 mg kg^{-1}, p.o.) were used as the reference standards. For the mechanistic study, FLU (8 mg kg^{-1}) and 2-PD (150 mg kg^{-1}) were intraperitoneally administered (i.p.) 10 min before drug administration.

Experimental animals. All animal-related procedures were performed according to the guidelines of the Institutional Animal Care and Use Committee of Pukyong National University (permission numbers: PKNUIACUC-2022-63, PKNUIACUC-2023-62, and PKNUIACUC-202405). For the pentobarbital-induced sleep test, we selected male ICR mice because this outbred strain has been widely used in drug screening models and shows relatively high sensitivity to hypnotics and sedatives, making it suitable for evaluating pharmacological efficacy such as sleep latency and duration.[11] The animals (3 weeks old, 20–25 g) were obtained from Koatech Co., Ltd (Pyeongtaek, Republic of Korea) and acclimated to the experimental animal housing facility for one week before use in the experiments. The animals were maintained under controlled conditions at 21 ± 2 °C with 55 ± 20% humidity, a 12 h light–dark cycle (lights on from 05:00 to 17:00), and an illumination range of 150–300 lux. For sleep architecture and sleep–wake profile analyses, we used male C57BL/6N mice (11 weeks old, 25–28 g), an inbred strain with low genetic variability that provides consistent EEG/EMG signals and stable circadian sleep–wake patterns, which are essential for reliable polysomnographic sleep analysis.[12] The animals were procured from Koatech Co., Ltd (Pyeongtaek, Republic of Korea) and acclimatized for one week in individually ventilated cages before use in the experiments. Housing conditions were maintained at 23 ± 2 °C with 55 ± 20% humidity. The other conditions were the same as those used for ICR mice. All mice used in this study had free access to food and water. Every effort was made to minimize discomfort and to use only the necessary number of animals to ensure reliable scientific results.

Pentobarbital-induced sleep test. Pentobarbital-induced sleep testing was performed after a single oral administration to assess acute sleep promoting effect. The experimental protocol and timeline for the test are illustrated in Fig. 1a. The test was conducted within a consistent time frame between 1:00 pm and 6:00 pm. Ten mice per group (n = 10) were used, and the mice were fasted for 24 h before the experiment. Fasting was extended to 24 h to minimize variability in gastrointestinal contents that could affect the absorption of the orally administered compounds and to enhance the sensitivity of the pentobarbital-induced sleep assay, as described in previous reports.[13,14]

All materials were administered orally (p.o.) 45 min before pentobarbital injection. The control group was treated with saline solution at a dose of 10 mL kg^{-1} instead of probiotics. Pentobarbital was administered intraperitoneally (i.p.) at a dose of 45 mg kg^{-1} (hypnotic dosage). After pentobarbital treatment, each mouse was transferred to a separate space, and sleep latency and duration were measured. Sleep latency was defined as the time elapsed until the loss of the righting reflex for at least one minute after intraperitoneal injection of pentobarbital, whereas sleep duration was defined as the time until the recovery of the righting reflex. Mice that did not exhibit sleep behavior within 10 min after pentobarbital administration were excluded. The observers who assessed these variables were blinded to the treatment groups.

Sleep architecture and sleep–wake profile analysis. For analysis targeting microbiota remodeling and EEG-defined sleep architecture, mice received once-daily oral gavage for 3 weeks. The experimental protocol and timeline for sleep architecture analysis are illustrated in Fig. 1b. Adult male C57BL/6N mice underwent chronic implantation of a head mount equipped with EEG and electromyography (EMG) electrodes to facilitate continuous polysomnographic monitoring.

The dorsal neck region of each mouse was shaved under deep pentobarbital anesthesia (50 mg kg^{-1}, i.p.), and the skin was disinfected with ethanol. A small incision was made to expose the skull, and the surgical site was carefully prepared to minimize tissue damage. The head mount (Pinnacle

Open Access Article. Published on 19 November 2025. Downloaded on 3/31/2026 6:45:20 AM.
This article is licensed under a Creative Commons Attribution 3.0 Unported Licence.

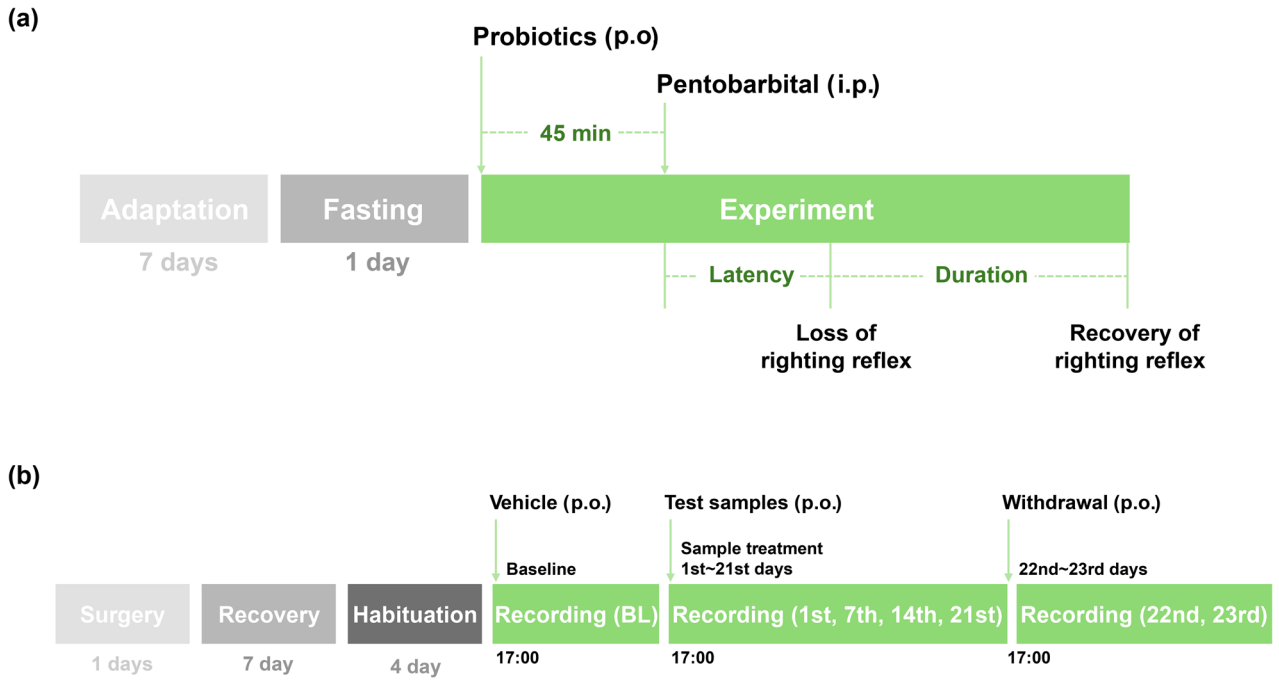

Fig. 1 Experimental designs for animal study. Protocol for the (a) pentobarbital-induced sleep test in ICR mice and (b) polysomnographic recordings during chronic administration in C57BL/6N mice. *Note*: p.o., per oral administration; i.p., intraperitoneal administration; BL, baseline.

Technology Inc., Lawrence, KS, USA) was positioned to align its front edge 3.0 mm anterior to the bregma. Four electrode screws were inserted into the skull to secure the EEG recordings, and two wire electrodes were implanted into the nuchal muscles for EMG recordings. The head mount was fixed to the skull using dental cement to ensure that it remained fixed throughout the study. After a one-week recovery period in individual cages after surgery, all animals were acclimated to the recording conditions for 3–4 days before the experiment. EEG and EMG signals were recorded using a slip-ring system to ensure that movement of the mice was unrestricted during data collection. Signal data were recorded using a Sirenia acquisition system (Pinnacle Technology Inc.), amplified (100-fold), and filtered (low-pass filter: 10 Hz). Finally, signals were stored at a sampling rate of 200 Hz. The sleep states were continuously monitored for 23 days, with the first day (day 0) used as the baseline. Recordings were obtained on days 1, 7, 14, and 21. Next, WD recording was conducted for two days. Baseline recordings were conducted for each animal for 24 h (beginning at 17:00) and were used as controls for the same animal. Mice were considered asleep when no significant EMG activity was recorded, and the data were classified into 10 epochs as REMS, NREMS, or awake using SleepSign ver. 3.0 (Kissei Comtec, Nagono, Japan). The bouts at each stage were defined as periods of one or more consecutive epochs (each epoch: 10 s). After probiotic administration, sleep latency was defined as the time required for the mice to enter NREMS for at least 120 s. Additionally, delta activity (0.5–4 Hz) was assessed during NREMS as the average percentage of delta power corresponding to NREMS.

Metabolomic analysis

Fecal metabolite extraction. Metabolites from the fecal samples were extracted for metabolomic analysis. Fecal samples were obtained from the sleep-architecture experiment at baseline (day 0, pre-dose) and day 21 (post-regimen) after a 3-week once-daily oral administration. For each 750 μL of sample, 2.25 mL of ice-cold methanol was added and vortexed for 1 min. After centrifugation at 11 500*g* for 10 min at 4 °C, the supernatant was collected and filtered through a 0.2 μm polyvinylidene fluoride (PVDF) syringe filter. Then, 100 μL of each sample was transferred into a 1.5 mL microtube for drying. The filtered samples were then dried using a vacuum concentrator (Eppendorf Concentrator plus™; Eppendorf, Hamburg, Germany).

Gas chromatography-mass spectrometry. Before gas chromatography-mass spectrometry (GC-MS) analysis, metabolites were derivatized by methoxyamine and trimethylsilylation. For methoxyamination, 10 μL of 40 mg mL^{-1} methoxyamine hydrochloride in pyridine (Sigma-Aldrich) was added to the dried metabolites and incubated for 90 min at 30 °C, with shaking at 1000 rpm. Subsequently, the metabolites were trimethylsilylated by adding 45 μL of *N*-methyl-*N*-trimethylsilyltrifluoroacetamide (Sigma-Aldrich) for 30 min at 37 °C, with shaking at 1000 rpm. GC-MS analysis was conducted using a Nexis GC-2030 system coupled to a GC-MS-QP2020 (Shimadzu, Kyoto, Japan), equipped with a SH-I-5Sil MS Cap column (30 m length, 0.25 mm i.d., and 0.25 μm film thickness). The chromatographic conditions and data analysis are detailed in the SI.

 This journal is © The Royal Society of Chemistry 2025

Open Access Article. Published on 19 November 2025. Downloaded on 3/31/2026 6:45:20 AM.
This article is licensed under a Creative Commons Attribution 3.0 Unported Licence.

Metagenomic analysis

Fecal microbiome analysis was conducted *via* full-length 16S rRNA gene sequencing. Samples were collected from the sleep-architecture cohort at two time points —baseline (day 0, pre-dose) and day 21 (post-regimen) —following a 3-week once-daily oral administration. Mouse fecal samples were used for genomic DNA extraction using the QIAamp PowerFecal Pro DNA kit (Qiagen, Hilden, Germany), following the manufacturer's instructions. DNA was eluted in 50 μL of elution buffer and stored at −20 °C until further processing. Genomic DNA (0.025–2.5 ng) extracted from mouse fecal samples was used as a template for the PCR amplification of the full-length 16S rRNA gene (V1–V9 regions). Each 50 μL PCR reaction contained 5 μL of gDNA, 2.5 μM barcoded universal primers (27F: 5′-AGRGTTYGATYMTGGCTCAG-3′ and 1492R: 5′-RGYTACCTTGTTACGACTT-3′), and the KAPA HiFi HotStart ReadyMix PCR kit (Roche, Basel, Switzerland). The thermal cycling conditions were as follows: initial denaturation at 95 °C for 3 min; 20 or 27 cycles at 95 °C for 30 s, 57 °C for 30 s, and 72 °C for 1 min; followed by a final extension at 72 °C for 1 min. The PCR products were quantified and size-verified using a 4200 TapeStation system (Agilent Technologies, Waldbronn, Germany) and normalized before pooling. Libraries were prepared using the SMRTbell Express Template Prep Kit 2.0 (Pacific Biosciences, Menlo Park, CA, USA) and sequenced on the PacBio Sequel II platform, with 10 h movie captures, according to the manufacturer's recommended protocol for full-length 16S amplicon sequencing. All sequencing procedures were performed by Theragenbio Bio (Seoul, Republic of Korea). Raw reads were processed into high-fidelity circular consensus sequences (HiFi reads) using the SMRT Link software. Adapter trimming was performed using Cutadapt (v3.2). Amplicon sequence variants (ASVs) were inferred using DADA2 (v1.18) in QIIME2 (v2022.2). Chimeric and low-quality sequences were excluded. Taxonomic classification was performed using the SILVA rRNA database (v138.99), optimized for long-read 16S sequences.

Statistical analysis

The results of all animal experiments are expressed as mean ± standard error of the mean (SEM). Statistical comparisons between each group and the control group were performed using one-way analysis of variance (ANOVA) with Dunnett's test. Significance levels are indicated by asterisks for results showing significance at $p < 0.05$ (*), $p < 0.01$ (**), and $p < 0.001$ (***). Significant differences between the two groups were evaluated using an unpaired Student's *t*-test. For paired comparisons across time points within the same group, the Student's paired *t*-test was used, with the following significance levels: $p < 0.05$ (#), $p < 0.01$ (##), and $p < 0.001$ (###). For additional unpaired comparisons between specific groups, the unpaired Student's *t*-test was used, with significance indicated by $p < 0.05$ (+) and $p < 0.001$ (+++).

All metabolomic statistical analyses were performed using R software (v4.4.1). sPLS-DA (mixOmics v6.30.0) with cross-validation was used to identify key metabolites (VIP ≥ 1), visualized as bar plots (ggplot2 v3.5.2). The results of hierarchical clustering (Ward's D^2, Euclidean distance) are presented as heatmaps (Pheatmap v1.0.12). ANOVA with Benjamini–Hochberg correction and Tukey's HSD (FDR $q < 0.05$) were applied; significant *p*-values are indicated on boxplots (ggpubr v0.6.0).

Alpha diversity (Chao1, Shannon, and Simpson) was calculated from rarefied ASV tables in QIIME2. Group differences were evaluated using the Wilcoxon rank-sum test in R and visualized with ggpubr. Beta diversity was assessed based on Bray–Curtis distances, non-metric multidimensional scaling (NMDS), and PERMANOVA. Taxonomy was classified from ASVs. Functional profiling was performed using PICRUSt2 (v2.4.1). Key taxa and functional genes were identified and ranked using Random Forest.

Results

Production of GABA by probiotic strains

Culture supernatants were analyzed using high-performance liquid chromatography to evaluate the GABA production capacity of the probiotic strains. The results demonstrated that GABA production differed significantly among the tested strains (Fig. 2a). *L. johnsonii* IDCC 9203 exhibited the highest concentration at 118.4 ± 5.6 mg L^{-1}, followed by *B. coagulans* IDCC 1201 (80.0 ± 6.2 mg L^{-1}) and *L. rhamnosus* IDCC 3201 (52.4 ± 8.1 mg L^{-1}). Several other strains, including *E. faecium* IDCC 2102, *L. casei* IDCC 3451, *L. reuteri* IDCC 3701, and *L. fermentum* IDCC 3901, showed moderate GABA production. Conversely, some strains, including *S. thermophilus* IDCC 2201, *L. salivarius* IDCC 3551, and *L. bulgaricus* IDCC 3601, did not produce detectable levels. GABA, a major inhibitory neurotransmitter involved in sleep regulation *via* the $GABA_A$ receptor pathway, was used as a marker to preliminarily assess the sleep-promoting potential of these strains.

Based on their high GABA production, *L. johnsonii* IDCC 9203, *B. coagulans* IDCC 1201, and *L. rhamnosus* IDCC 3201 were selected as promising candidates for further study. To characterize *B. coagulans* IDCC 1201, its GABA production was assessed under glutamate-supplemented conditions. *B. coagulans* IDCC 1201 produced 14.81 ± 0.94 mg L^{-1} GABA, with a glutamate to GABA conversion rate of 42.26 ± 2.69% (Fig. 2b). This result indicates that *B. coagulans* IDCC 1201 synthesizes a considerable amount of GABA and efficiently utilizes available glutamate. The combination of high GABA production and efficient conversion suggests that this strain is a strong candidate for probiotic applications targeting GABA-related physiological functions, such as sleep regulation.

Effects of probiotic strains on sleep latency and sleep duration

The sleep-promoting potential of the probiotic strains was evaluated using the pentobarbital-induced sleep test. Administration of *L. johnsonii* IDCC 9203, *B. coagulans* IDCC 1201, and *L. rhamnosus* IDCC 3201 (1×10^8 CFU per day) sig-

Open Access Article. Published on 19 November 2025. Downloaded on 3/31/2026 6:45:20 AM.
This article is licensed under a Creative Commons Attribution 3.0 Unported Licence.

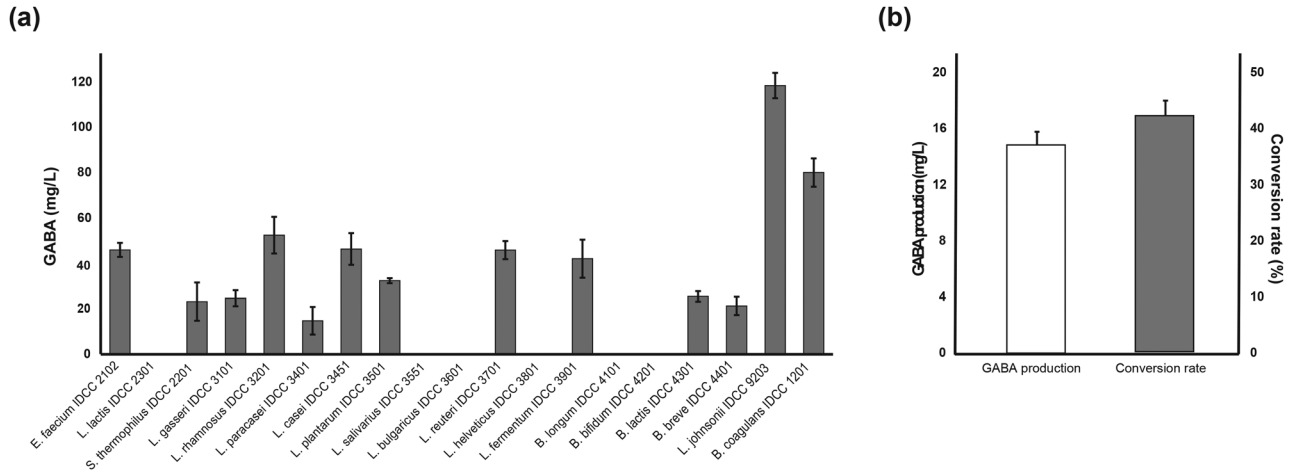

Fig. 2 GABA production and conversion efficiency of *B. coagulans* IDCC 1201. (a) GABA production (mg L^{-1}) of probiotic strains. (b) GABA production and glutamate-to-GABA conversion rate in *B. coagulans* IDCC 1201. Data are mean ± SD. The experiments of 2a and 2b derive from independent experimental runs conducted on different days under the same medium, protocol, and sampling time; absolute GABA concentrations (mg L^{-1}) are not directly comparable between panels (n = 3).

nificantly reduced sleep latency compared to that in the control group (69.1 ± 6.1 min) (Fig. 3a). Among the tested strains, *B. coagulans* IDCC 1201 exerted the most pronounced effect on sleep duration, significantly increasing it to 92.0 ± 6.3 min (Fig. 3b), whereas *L. johnsonii* IDCC 9203 and *L. rhamnosus* IDCC 3201 had no significant effect on sleep duration.

Dose-dependent sleep-promoting effect of *B. coagulans* IDCC 1201

As *B. coagulans* IDCC 1201 showed the strongest sleep-promoting effect, its dose-dependent impact was evaluated at 0.5, 1, 10, and 20 × 10^8 CFU per day. Sleep latency was significantly reduced at all doses, except 0.5 × 10^8 CFU per day, compared to that in the control (Fig. 3c). However, no significant differences were observed between the effective doses, suggesting a plateau effect at 1 × 10^8 CFU per day. Sleep duration was significantly increased at all doses except for 0.5 × 10^8 CFU per day (Fig. 3d). Notably, the highest dose did not further enhance sleep duration compared to 1 × 10^8 CFU per day, indicating a saturation effect.

Mechanistic investigation of *B. coagulans* IDCC 1201-induced sleep enhancement

To investigate whether *B. coagulans* IDCC 1201 induces sleep *via* the $GABA_A$-BZD receptor, we conducted pentobarbital-induced sleep experiments using ZPD, a BZD site agonist, and FLU, a BZD site antagonist. The sleep-promoting effect of ZPD was completely blocked by coadministration with FLU, supporting its action *via* the $GABA_A$-BZD receptor (Fig. 4). Similarly, the sleep-promoting effect of *B. coagulans* IDCC 1201 was inhibited by FLU, indicating that it acts at the same site (Fig. 4b). At 1 × 10^9 CFU per day (supramaximal dose), sleep latency plateaued, and coadministration with FLU or 2-PD did not significantly alter latency (Fig. 4a). To assess the involvement of the H_1 receptor, another experiment was conducted using DH, an H_1 receptor antagonist, and 2-PD, an H_1 receptor agonist. Coadministration of DH and 2-PD abolished the effect of DH, confirming its dependence on the H1 receptor (Fig. 4). In contrast, the sleep-promoting effect of *B. coagulans* IDCC 1201 remained unchanged in the 2-PD group, suggesting that the histaminergic pathway was not involved (Fig. 4b).

These results demonstrate that *B. coagulans* IDCC 1201 enhances sleep *via* the BZD site of the $GABA_A$ receptor and not through the histamine H_1 receptor, indicating a GABAergic mechanism of action.

Effect of chronic administration of *B. coagulans* IDCC 1201 on sleep latency and sleep duration

To evaluate both the quantity and quality of sleep, EEG and EMG recordings were conducted following a 3-week administration of *B. coagulans* IDCC 1201. This allowed the assessment of potential side effects, such as tolerance or WD. Sleep latency in the *B. coagulans* IDCC 1201 group ranged from approximately 26 min on day 1 to 15 min on day 21 (Fig. 5a). A significant reduction was observed over time (day 1, $p < 0.05$; days 7, 14, and 21, $p < 0.01$). ZPD significantly reduced sleep latency throughout the treatment period (day 1: $p < 0.001$; days 7 and 14: $p < 0.01$; day 21: $p < 0.05$), but its effect gradually weakened. While days 7 and 14 showed no significant changes from day 1, sleep latency increased significantly on day 21, indicating the development of tolerance. On day 1, *B. coagulans* IDCC 1201 showed a slightly longer sleep latency than ZPD, but by day 21, no significant difference was observed between the groups. During the WD period, both groups returned to baseline values similar to those of the control group.

 This journal is © The Royal Society of Chemistry 2025

Open Access Article. Published on 19 November 2025. Downloaded on 3/31/2026 6:45:20 AM.
This article is licensed under a Creative Commons Attribution 3.0 Unported Licence.

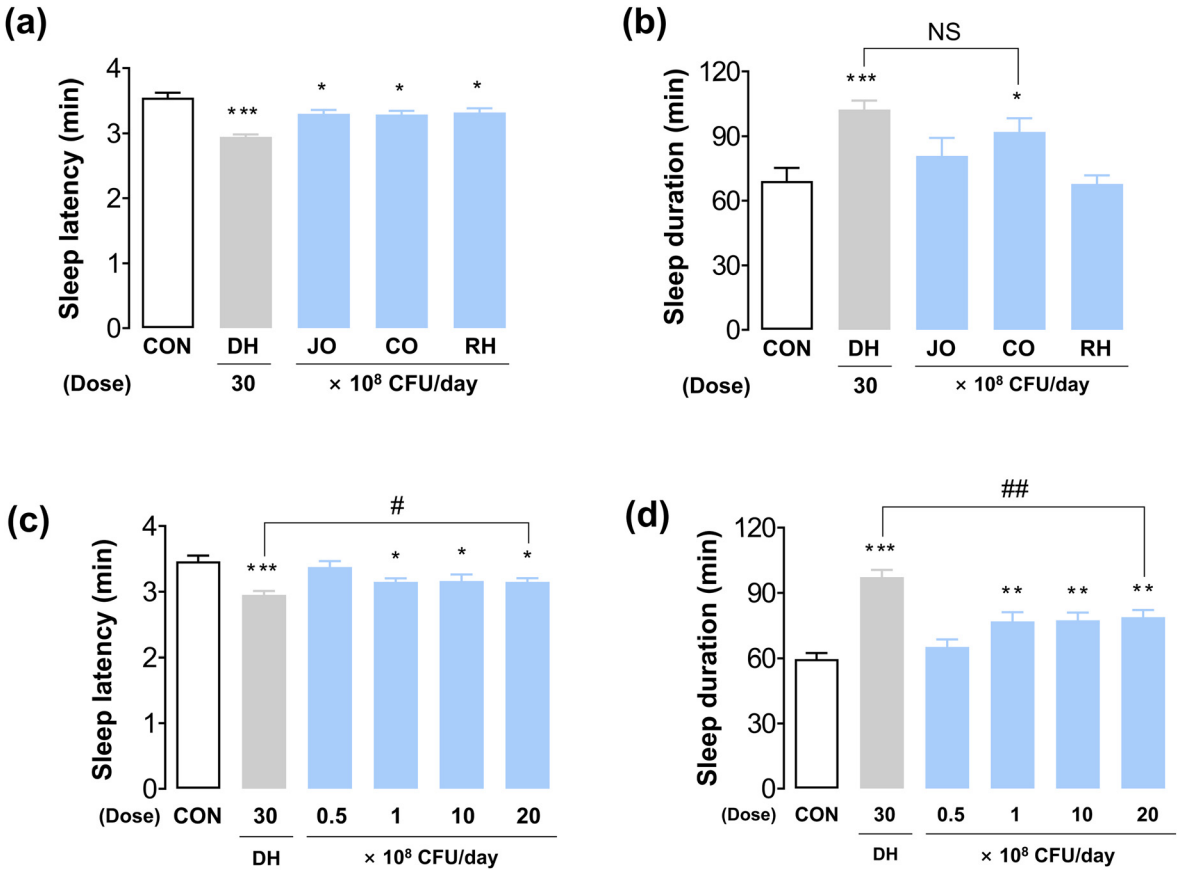

Fig. 3 Effects of *B. coagulans* IDCC 1201 on pentobarbital-induced sleep latency and duration in mice. (a) Sleep latency and (b) duration measured after administration of probiotic strains. (c and d) Dose-dependent effects of *B. coagulans* IDCC 1201 at 0.5, 1, 10, and 20 × 10^8 CFU per day. Each column represents mean ± SEM (n = 10). * $p < 0.05$, *** $p < 0.001$ *vs.* control (Dunnett's test); # $p < 0.05$, ## $p < 0.01$ *vs.* DH (Student's t-test). *Note*: CON, control group; DH, doxepin hydrochloride group; JO, *Lactobacillus johnsonii* IDCC 9203-probiotics group; CO, *Bacillus coagulans* IDCC 1201-probiotics group; RH, *Lactobacillus rhamnosus* IDCC 3201-probiotics group; NS, not significant.

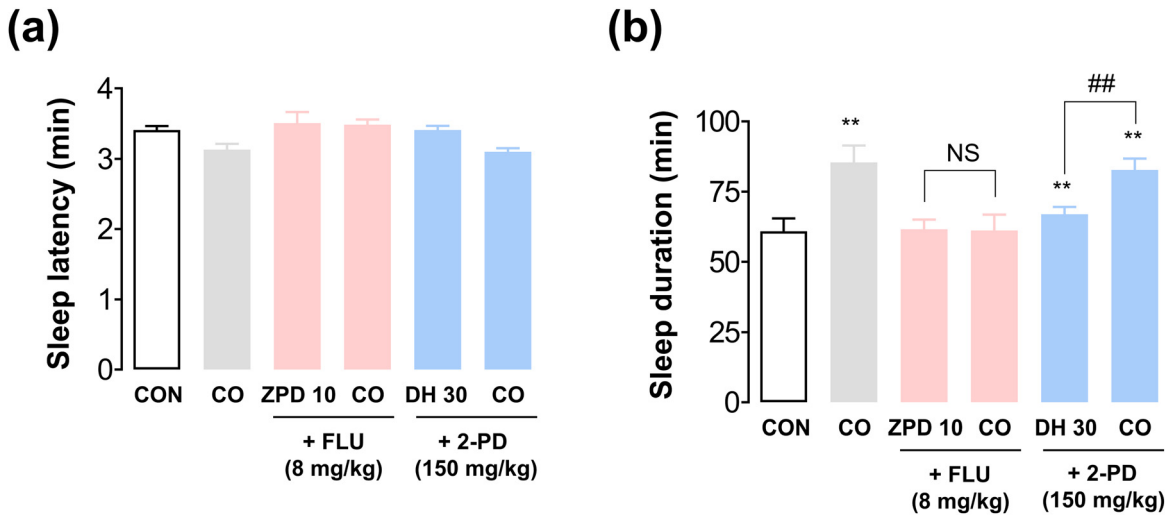

Fig. 4 Effects of the FLU and 2-PD on the changes in sleep latency and sleep duration in mice treated with *B. coagulans* IDCC 1201, ZPD, and DH. (a) Sleep latency and (b) sleep duration measured following administration of CO 10^9 CFU per day, ZPD 10 mg kg^{-1}, or DH 30 mg kg^{-1}, with FLU or 2-PD administered 15 min prior. Each column represents mean ± SEM (n = 10). ** $p < 0.01$ *vs.* CON (Dunnett's test). ## $p < 0.01$ ZPD/DH *vs.* CO (Student's t-test). *Note*: 2-PD, 2-pyridylethylamine dihydrochloride group; CO, *Bacillus coagulans* IDCC 1201-probiotics group; CON, control group; DH, doxepin hydrochloride group; FLU, flumazenil; NS, not significant; ZPD, zolpidem.

Open Access Article. Published on 19 November 2025. Downloaded on 3/31/2026 6:45:20 AM.
This article is licensed under a Creative Commons Attribution 3.0 Unported Licence.

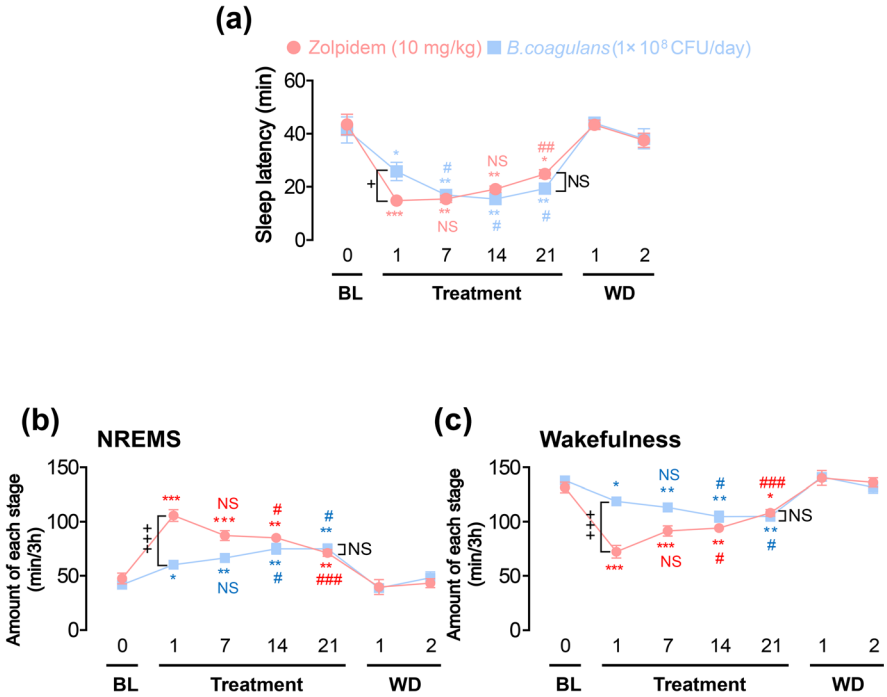

Fig. 5 Effects of chronic administration of ZPD and *B. coagulans* IDCC 1201 on sleep latency, NREMS, and wakefulness. (a) Sleep latency, (b) NREMS, and (c) wakefulness measured during chromic administration of ZPD and *B. coagulans* IDCC 1201. Each dot and box represent mean ± SEM (n = 8). * $p < 0.05$, ** $p < 0.01$, *** $p < 0.001$ *vs.* BL (Dunnett's test); # $p < 0.05$, ## $p < 0.01$, ### $p < 0.001$ *vs.* day 1 (paired Student's t-test); + $p < 0.05$, +++ $p < 0.001$ *vs.* ZPD (unpaired Student's t-test). *Note*: BL, baseline; NS, not significant; SEM, standard error of the mean; WD, withdrawal; ZPD, zolpidem; NREMS, non-rapid eye movement sleep.

Fig. 5b and c show the cumulative amounts of NREMS and wakefulness during the first 3 h after the administration of *B. coagulans* IDCC 1201 and ZPD. In the *B. coagulans* IDCC 1201 group, NREMS duration was 60.2 ± 3.0 min on day 1 and gradually increased to 66.4 ± 4.0 min on day 7, reaching 74.9 ± 4.9 min by days 14 and 21. This sustained and statistically significant increase indicated a gradual improvement in sleep architecture. In contrast, NREMS in the ZPD group started at 105.7 ± 5.4 min on day 1 but showed a gradual decline with significant reductions on days 14 ($p < 0.05$) and 21 ($p < 0.001$). Although a significant difference was observed between the two groups on day 1 ($p < 0.001$), no significant difference was observed on day 21. The amount of wakefulness in both groups followed an inverse trend to that of the NREMS.

Temporal changes in sleep architecture following *B. coagulans* IDCC 1201 administration

To investigate the temporal effects of *B. coagulans* IDCC 1201 on sleep architecture, sleep stages were analyzed over a 24 h period (Fig. 6a). Continued administration led to a gradual increase in the duration of NREMS. On day 1, a significant increase was observed only during the first hour ($p < 0.05$). By day 7, this effect had been extended to the first 2 h (1st, $p < 0.01$; 2nd, $p < 0.05$). On days 14 and 21, NREMS significantly increased during the first 3 h (day 14: 1st to 2nd, $p < 0.01$; 3rd, $p < 0.05$; day 21: 1st to 2nd, $p < 0.05$; 3rd, $p < 0.01$). Additionally, notable improvements were observed during both the nighttime and daytime periods. However, no significant changes were detected during the WD period, indicating the absence of residual or prolonged effects after treatment cessation.

Modulation of sleep–wake episodes by *B. coagulans* IDCC 1201

To assess the effects of *B. coagulans* IDCC 1201 on sleep–wake architecture, we analyzed the mean duration and frequency of NREMS and wakefulness episodes over 24 h. On day 1, ZPD reduced the mean wakefulness duration by 68.2%; however, this effect diminished over time. In contrast, *B. coagulans* IDCC 1201 showed a smaller initial reduction (29.2%), which progressively increased and remained significant through days 7, 14, and 21. Neither treatment affected the mean NREMS duration, and no changes were observed during the WD period (Fig. 7a and b).

The frequency of NREMS bouts increased significantly in the ZPD group from day 1, but this effect weakened over time. *B. coagulans* IDCC 1201 did not affect the bout frequency on day 1; however, a gradual increase was observed from day 7 onward, with a significant increase by day 21 (Fig. 7c and d). Wakefulness bout frequency showed similar trends in both groups, with no changes in the WD phase.

Stage transition analysis within the first 3 h post-administration revealed increased NREMS-wake transitions in both

 This journal is © The Royal Society of Chemistry 2025

Open Access Article. Published on 19 November 2025. Downloaded on 3/31/2026 6:45:20 AM.
This article is licensed under a Creative Commons Attribution 3.0 Unported Licence.

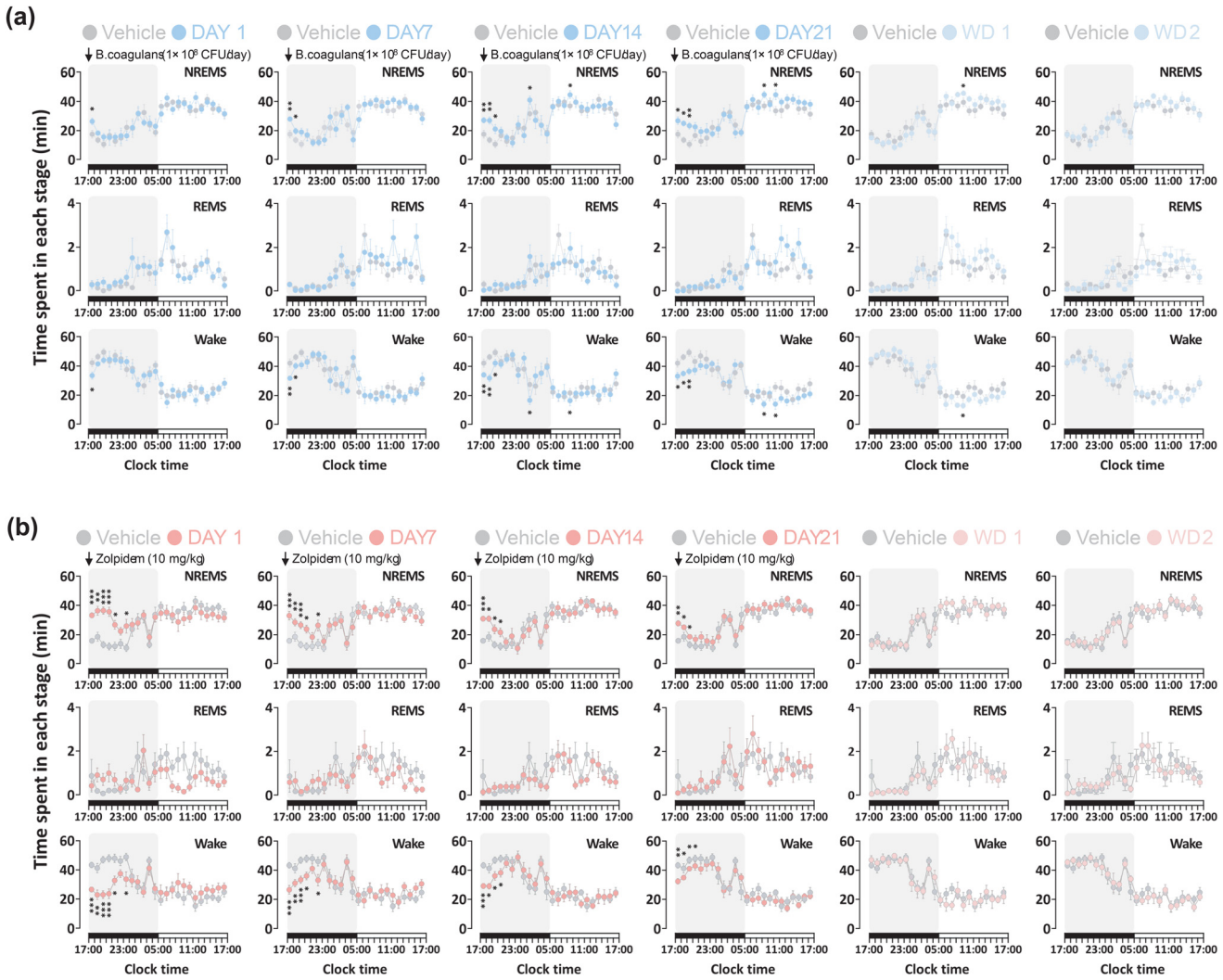

Fig. 6 Time-course changes in sleep architecture during chronic administration and withdrawal of *B. coagulans* IDCC 1201 and ZPD. Hourly sleep stage changes measured during chronic administration and withdrawal. (a) *B. coagulans* IDCC 1201 group: gray circles, baseline (vehicle); blue circles, *B. coagulans* IDCC 1201 administration; light blue circles, withdrawal day. (b) ZPD group: grey circles, baseline (vehicle); red circles, ZPD administration; light red circles, withdrawal day. Each data point represents the hourly mean ± SEM (n = 8). *p < 0.05, **p < 0.01, ***p < 0.001 *vs.* control group (paired Student's t-test). *Note*: NREMS, non-rapid eye movement sleep; SEM, standard error of the mean; WD, withdrawal; ZPD, zolpidem.

groups. Although ZPD induced changes from day 1, *B. coagulans* IDCC 1201 showed effects from day 7 onward. Transitions involving the REMS remained unchanged, and none of the groups showed any residual effects during the WD period (Fig. 8a).

Distribution analysis of episode duration showed that ZPD consistently increased short NREMS episodes (0–120 s) at all time points. *B. coagulans* IDCC 1201 induced a similar but delayed effect, with a significant increase from day 7 onwards. Both treatments increased short-duration episodes of wakefulness, suggesting the fragmentation of prolonged wakefulness and the promotion of more stable sleep. Collectively, these results demonstrate that, although ZPD exerts immediate but transient effects, *B. coagulans* IDCC 1201 gradually enhances sleep quality over time without inducing WD, supporting its potential as a long-term sleep-modulating agent.

Analysis of delta activity following *B. coagulans* IDCC 1201 administration

Delta activity serves as an indicator of sleep depth and intensity and is commonly used to evaluate sleep quality during NREMS.[15] ZPD administration resulted in a significant reduction in delta activity from day 1 to 21 (p < 0.05), suggesting that while ZPD enhances sleep, its efficacy weakens over time, potentially leading to a decline in sleep quality. In contrast, *B. coagulans* IDCC 1201 administration did not induce any significant changes in delta activity throughout the treatment period, maintaining a pattern similar to that of the

Open Access Article. Published on 19 November 2025. Downloaded on 3/31/2026 6:45:20 AM.
This article is licensed under a Creative Commons Attribution 3.0 Unported Licence.

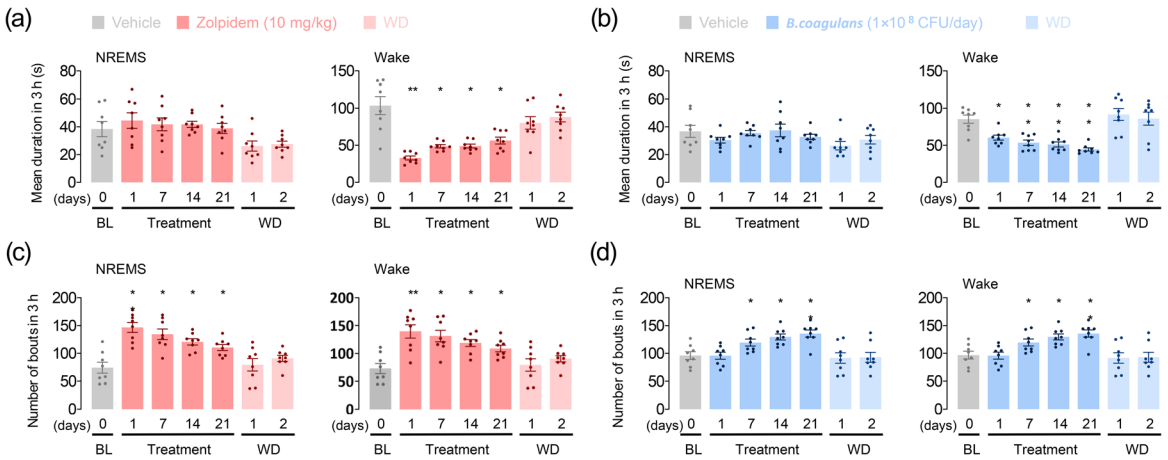

Fig. 7 Features of sleep–wake bouts during chronic administration of ZPD and *B. coagulans* IDCC 1201. Changes in mean duration of (a) NREMS and (b) wakefulness and number of bouts of (c) NREMS and (d) wakefulness during 3 h following treatment. Every column represents the hourly mean ± SEM (n = 8). * $p < 0.05$, ** $p < 0.01$, *** $p < 0.001$ *vs.* control (Dunnett's test). *Note*: BL, baseline; NREMS, non-rapid eye movement sleep; SEM, standard error of the mean; WD, withdrawal; ZPD, zolpidem.

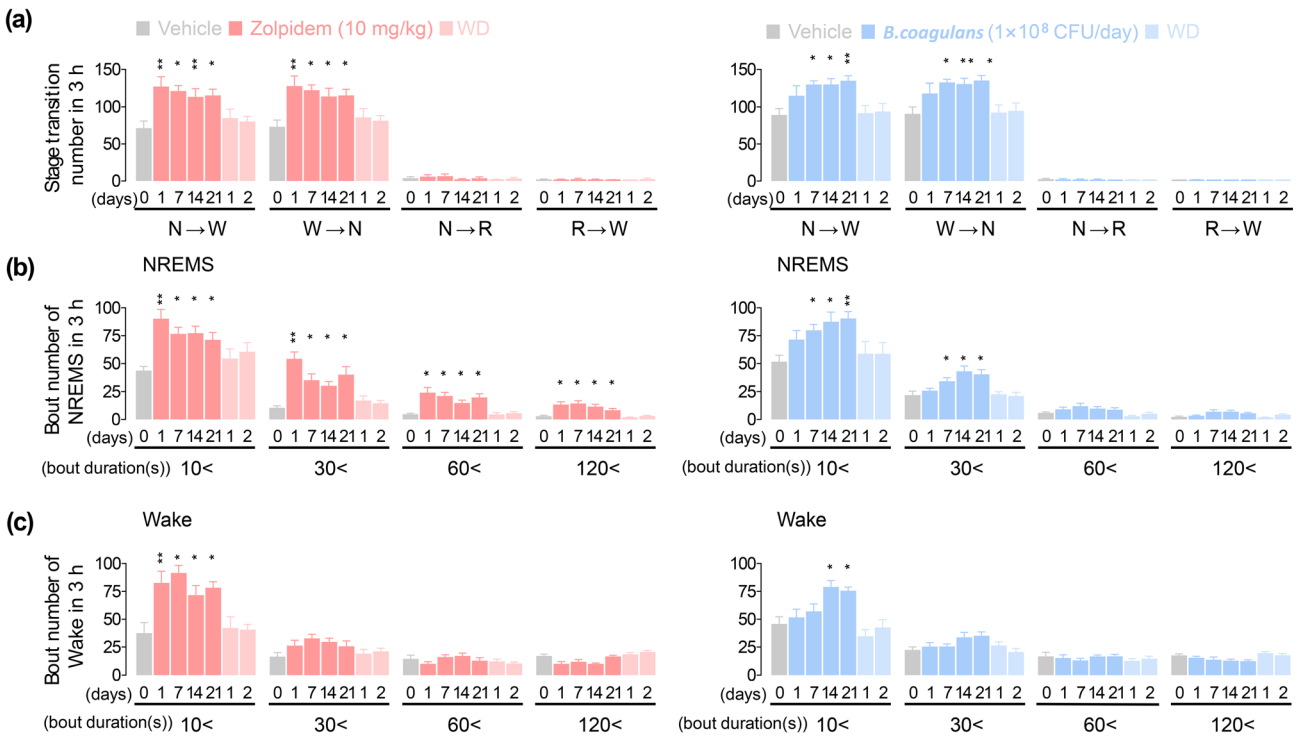

Fig. 8 Effects of chronic administration and withdrawal of ZPD and *B. coagulans* IDCC 1201 on sleep stage transitions, NREMS episodes, and wakefulness. (a) Number of stage transitions; (b) number of NREMS episodes; (c) number of wakefulness episodes during 3 h after treatment during chronic administration. Every column represents the hourly mean ± SEM (n = 8). * $p < 0.05$, ** $p < 0.01$, *** $p < 0.001$ *vs.* control (Dunnett's test). *Note*: BL, baseline; NREMS, non-rapid eye movement sleep; SEM, standard error of the mean; Wake, wakefulness; WD, withdrawal; ZPD, zolpidem.

control group (Fig. 9). These findings indicate that *B. coagulans* IDCC 1201 improves sleep efficiency over time and preserves sleep quality by promoting physiological sleep without altering sleep depth. Following the cessation of administration, both groups exhibited normal sleep patterns without any residual effects, confirming the absence of WD-related disturbances.

Fecal metabolomic profiles following *B. coagulans* IDCC 1201 administration

Fecal metabolomic profiling using GC-MS revealed distinct separation between the treatment and control groups in the sPLS-DA model, with VIP-selected metabolites (VIP > 1.0) contributing most to this discrimination (Fig. 10a and b).

 This journal is © The Royal Society of Chemistry 2025

Open Access Article. Published on 19 November 2025. Downloaded on 3/31/2026 6:45:20 AM.
This article is licensed under a Creative Commons Attribution 3.0 Unported Licence.

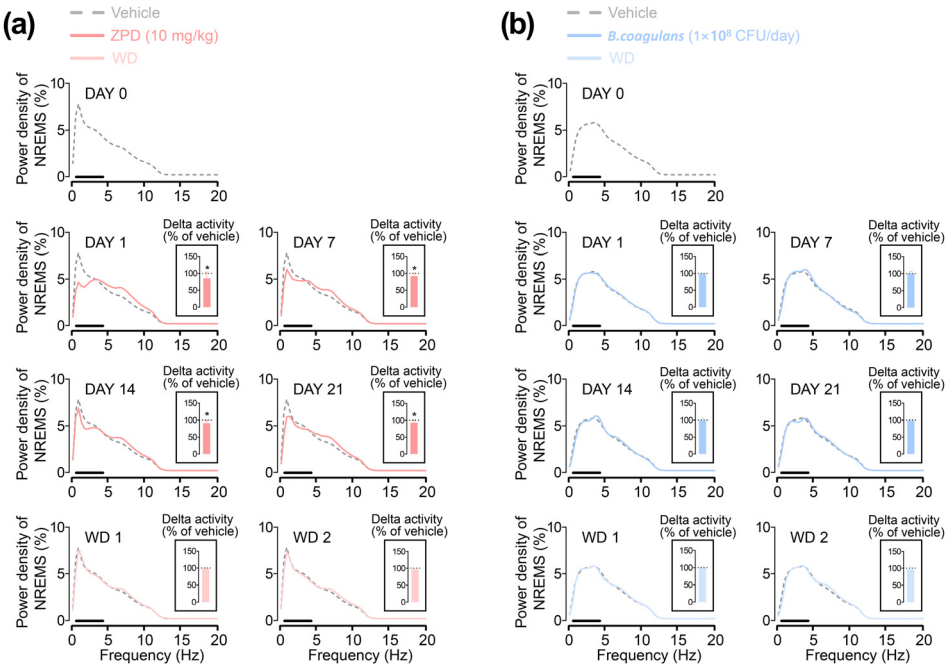

Fig. 9 Effects of ZPD and *B. coagulans* IDCC 1201 on EEG delta power during NREMS. EEG delta power density curves during NREMS with (a) ZPD and (b) *B. coagulans* IDCC 1201 administration. Grey curves: baseline (vehicle); red and blue curves: ZPD and *B. coagulans* IDCC 1201 administration; light red and blue curve: withdrawal days. The solid bar indicates the delta wave range (0.5–4 Hz). * $p < 0.05$ *vs.* control (paired Student's *t*-test). *Note*: NREMS, non-rapid eye movement sleep; SEM, standard error of the mean; wake, wakefulness; WD, withdrawal; ZPD, zolpidem.

Heatmap analysis indicated significant alterations in metabolites related to energy metabolism, neurotransmission, and oxidative stress regulation (Fig. 10c). The treatment group showed marked reductions in tricarboxylic acid (TCA) cycle intermediates (fumaric, pyruvic, and aspartic acids; Fig. 10d–f) and excitatory amino acids (serine, threonine, and glutamic acid; Fig. 10g–i). In contrast, levels of neuromodulatory metabolites (4-hydroxyphenylacetate, 5-hydroxyindole-3-acetic acid, cortol, and sitosterol; Fig. 10j–m) and alpha-tocopherolacetate (Fig. 10n and o) were elevated, while gamma-tocopherol was reduced.

Gut microbiome diversity and composition following *B. coagulans* IDCC 1201 administration

To evaluate the impact of *B. coagulans* IDCC 1201 on the gut microbial composition, taxonomic profiling was conducted using fecal samples. Alpha-diversity analysis revealed that the *B. coagulans* IDCC 1201 group exhibited a significantly higher microbial richness than that in the vehicle group, as indicated by higher Chao1 ($p < 0.028$) and observed ($p < 0.014$) values (Fig. 11a and b). In contrast, the ZPD-treated group showed a significant reduction in microbial evenness, as assessed using Shannon ($p < 0.008$) and Simpson indices ($p < 0.032$), indicating ZPD-induced dysbiosis (Fig. 11c and d). Beta-diversity analysis using NMDS and PERMANOVA demonstrated a significant difference in microbial composition between the *B. coagulans* IDCC 1201 and ZPD-treated groups (FDR = 0.027). In contrast, no significant differences were observed between vehicle and treatment groups (Fig. 11e). These findings suggest that *B. coagulans* IDCC 1201 induces a distinct microbial shift compared to ZPD while preserving the baseline structure of the gut microbiota. At the species level, administration of *B. coagulans* IDCC 1201 significantly increased the relative abundance of *B. coagulans* compared to that in the vehicle group and led to significantly higher levels of *Bacillus coagulans*, *Lactobacillus murinus*, and *Candidatus* Arthromitus than those in the ZPD group (Fig. 11f–h). These taxa have been previously associated with gut–brain axis modulation or immunoregulatory functions. Conversely, ZPD administration resulted in the enrichment of *Lachnospiraceae* bacterium, as consistently identified using both taxonomic profiling and Random Forest classification (Fig. 11i). These microbial shifts may reflect an imbalance in the gut ecosystem associated with pharmacologically induced sedation. Furthermore, Random Forest models confirmed that *B. coagulans* and *L. murinus* were strong discriminative taxa for the *B. coagulans* IDCC 1201 group, whereas *L. johnsonii* and *Lachnospiraceae* bacterium served as key classifiers for the ZPD group (Fig. 11j and k).

Functional gene profiles following *B. coagulans* IDCC 1201 administration

Functional gene prediction using PICRUSt2 identified several genes associated with sleep-related metabolic pathways. These genes were categorized into glutamate- and putrescine-related pathways. In the putrescine pathway, the relative expression of K01581 (*speC*, *speF*), which encodes ornithine decarboxylase, was significantly lower in the ZPD group than in the vehicle group ($p < 0.016$) (Fig. 12a). Conversely, the expression of

Open Access Article. Published on 19 November 2025. Downloaded on 3/31/2026 6:45:20 AM.
This article is licensed under a Creative Commons Attribution 3.0 Unported Licence.

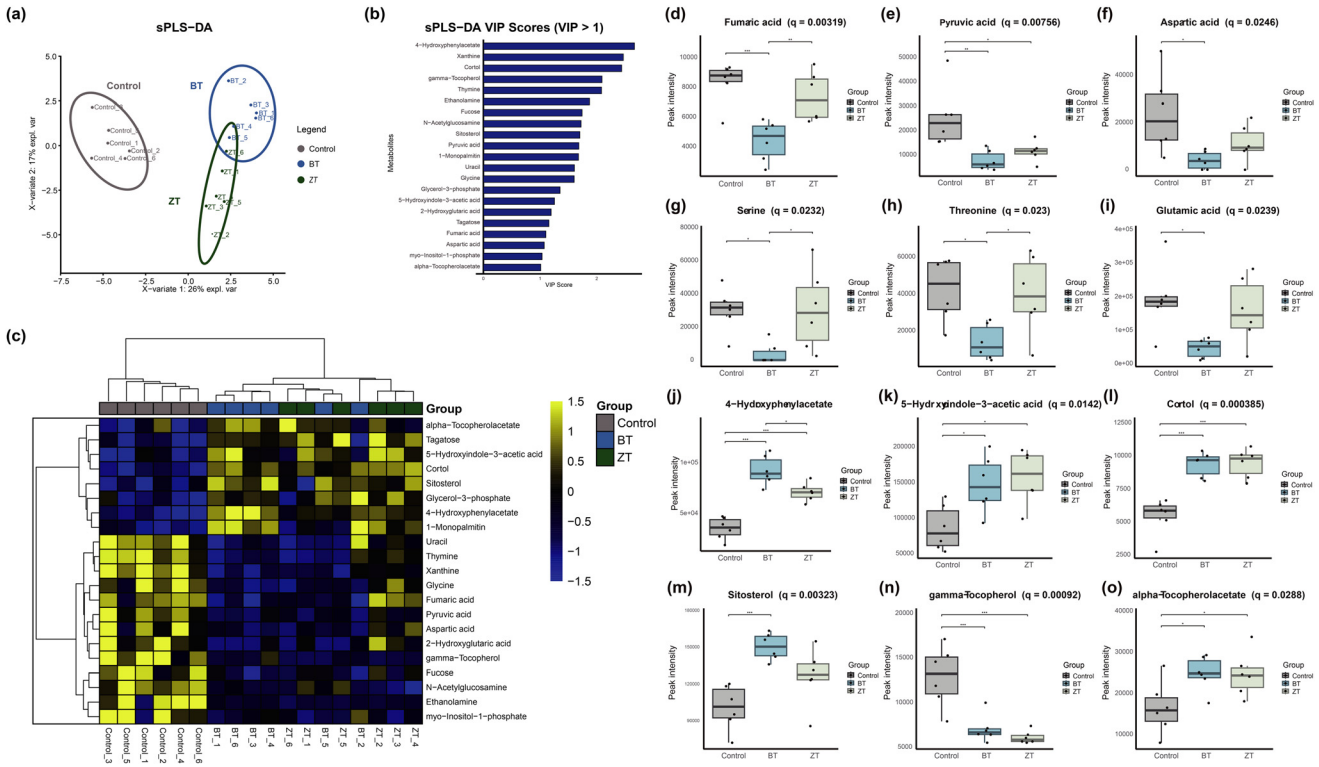

Fig. 10 Fecal metabolomic profiling and representative metabolite comparisons following administration of *B. coagulans* IDCC 1201 and zolpidem. (a) sPLS-DA score plot showing distinct clustering of CON, BT and ZT groups based on fecal metabolite profiles; (b) bar plot of metabolites with VIP scores ≥1 contributing to group separation; (c) heatmap of *z*-score-normalized intensities of selected metabolites. (d–o) Box plots showing peak intensities of selected metabolites: (d) fumaric acid, (e) pyruvic acid, (f) aspartic acid, (g) serine, (h) threonine, (i) glutamic acid, (j) 4-hydroxyphenylacetate, (k) 5-hydroxyindole-3-acetic acid, (l) cortol, (m) sitosterol, (n) γ-tocopherol, and (o) α-tocopherol acetate. Data are expressed as individual values with median and interquartile ranges (n = 6 per group). *p < 0.05, **p < 0.01, ***p < 0.001 (one-way ANOVA with Benjamini–Hochberg correction; Tukey's HSD post HSD test). *Note*: CON, control group; BT, *Bacillus coagulans* IDCC 1201-treated group; ZT, zolpidem-treated group.

K09251 (*patA*), which encodes a putrescine transaminase, was significantly higher in the ZPD group (p < 0.008) (Fig. 12b).

In the glutamate-related pathway, the expression of K09681 (*gltC*), a transcriptional regulator of the glutamate operon, was significantly elevated in the *B. coagulans* group (p < 0.048) (Fig. 12c). The expression of K07250 (*gabT*), which encodes 4-aminobutyrate aminotransferase, was significantly lower in the ZPD group than in the *B. coagulans* group (p < 0.008), with a decreasing trend compared to that in the vehicle group (Fig. 12d). Additionally, K00270 (*pdh*), which is involved in aromatic amino acid metabolism and TCA cycle activity, and K09682 (*hpr*), which encodes a MarR family transcriptional regulator related to redox regulation, were significantly upregulated in the *B. coagulans* group (p < 0.048 and p < 0.016, respectively) (Fig. 12e and f).

Discussion

This study systematically evaluated the sleep-promoting properties of various probiotic strains, with a particular emphasis on *B. coagulans* IDCC 1201. Initially, we evaluated GABA production and observed marked variability. *L. johnsonii* IDCC 9203, *B. coagulans* IDCC 1201, and *L. rhamnosus* IDCC 3201 showed the highest production levels. As GABA is a key inhibitory neurotransmitter involved in sleep regulation through the $GABA_A$ receptor pathway, the ability of certain probiotic strains to produce GABA has significant relevance for enhancing sleep.[16] *B. coagulans* IDCC 1201 exhibited high GABA production and showed a high GABA conversion rate, suggesting efficient glutamate-to-GABA transformation. This is particularly important because both total GABA output and metabolic efficiency may contribute to functional outcomes. However, *in vitro* GABA productivity did not predict the outcome of the acute pentobarbital assay. This experiment detects immediate, single-dose sleep promoting effects and depends more on the bioavailability of strain-derived bioactive and their receptor-level actions than on GABA amounts. The absence of an acute effect with *L. johnsonii* despite high *in vitro* GABA production, suggests mechanisms that likely require repeated dosing—*e.g.*, colonization within *in situ* production, substrate availability, and/or microbiota remodeling.

Moreover, *B. coagulans* IDCC 1201 possesses spore-forming ability, which confers enhanced gastrointestinal stability and viability.[17] These dual characteristics advance its therapeutic potential as a functional probiotic for sleep modulation.

 This journal is © The Royal Society of Chemistry 2025

Open Access Article. Published on 19 November 2025. Downloaded on 3/31/2026 6:45:20 AM.
This article is licensed under a Creative Commons Attribution 3.0 Unported Licence.

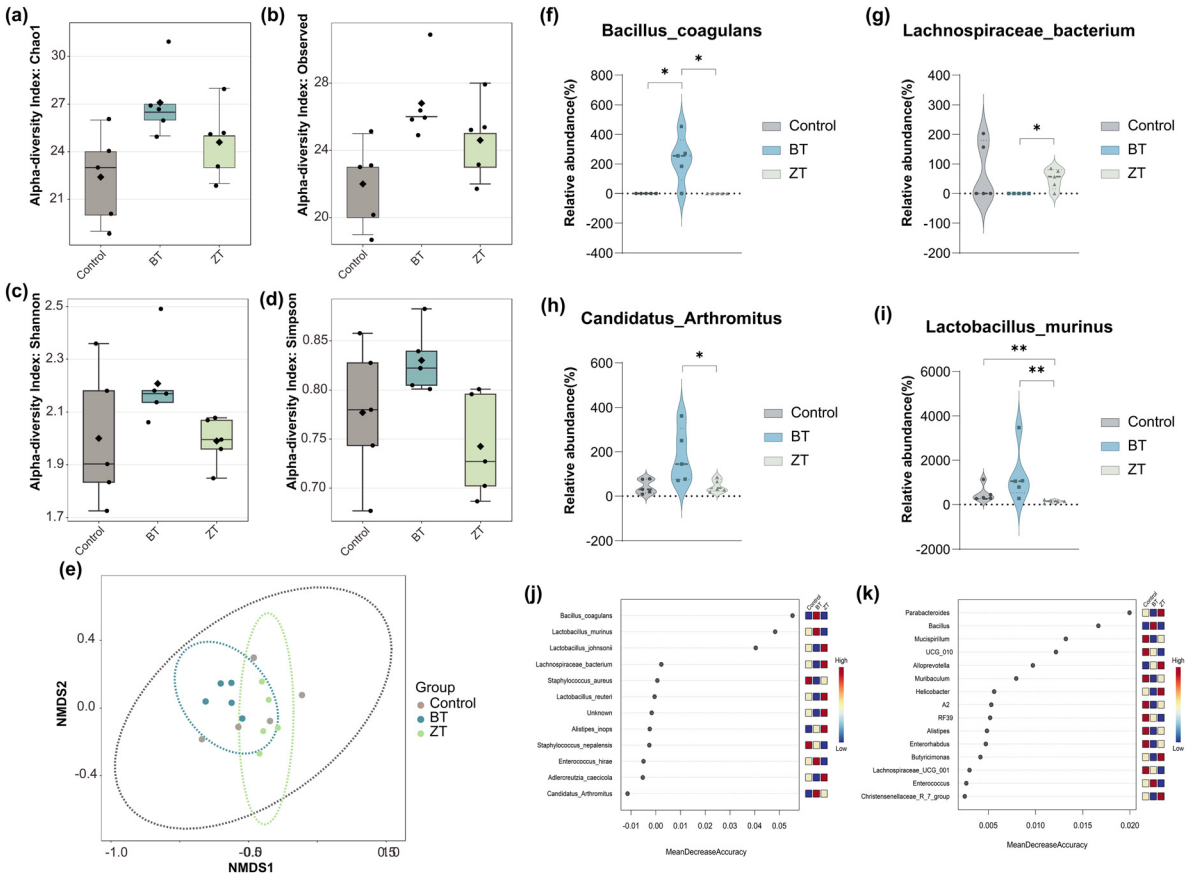

Fig. 11 Comparison of gut microbiome diversity, composition, and classification analysis. (a–d) Alpha diversity indices including Chao1 index, observed features, Shannon index, and Simpson index. (e) Beta diversity visualized by non-metric multidimensional scaling (NMDS) plot based on Bray–Curtis distance. (f–i) Relative abundances of representative microbial taxa at the species level, including *Bacillus coagulans*, *Lachnospiraceae* bacterium, *Candidatus* Arthromitus, and *Lactobacillus murinus*, shown as box plots comparing the groups. (j and k) Top discriminatory taxa identified by Random Forest classification differentiating the groups. Significant differences between groups are indicated as $*p < 0.05$, $**p < 0.01$, $***p < 0.001$ (Mann–Whitney *U* test). *Note*: CON, control group; BT, *Bacillus coagulans* IDCC 1201-treated group; ZT, zolpidem-treated group.

In the pentobarbital-induced sleep model, *B. coagulans* IDCC 1201 demonstrated the highest efficacy, significantly reducing sleep latency and uniquely increasing total sleep duration among the tested strains. The improvement in both sleep latency and duration indicates more sleep and better regulation of the neurophysiological processes that control sleep onset and maintenance. Dose–response analysis revealed a saturation effect at 1×10^8 CFU per day, with no further benefits observed at higher doses. This suggests that the maximal efficacy can be achieved at relatively low dosages. Prolonged administration or high-dose intake of various anxiolytics and antidepressants, including BZDs and Z-drugs, has been associated with an increased risk of adverse effects, such as overdose, falls and fractures, infections, and dementia.[18] In contrast, this finding is advantageous for minimizing potential adverse effects and enhancing its applicability in clinical and consumer settings.

Sleep regulation involves various mechanisms related to sleep induction, including the GABA, histamine, serotonin, and adenosine pathways,[19] among which the $GABA_A$ receptor-mediated mechanism is the most well-established.[20] Among the multiple binding sites present on the $GABA_A$ receptor, the GABA-BZD binding sites are particularly well known for their critical roles in sleep regulation. The BZD site of the $GABA_A$ receptor acts as an allosteric modulator that promotes neuronal inhibition and facilitates sleep.[21] Mechanistic investigations revealed that *B. coagulans* IDCC 1201 exerts sleep-promoting effects through the GABAergic system, specifically *via* the BZD site of the $GABA_A$ receptor, as evidenced by the complete loss of efficacy upon FLU coadministration.[22] Although this mechanism is similar to that of ZPD, *B. coagulans* IDCC 1201 shows a clear distinction by maintaining stable delta activity throughout the treatment period. Electroencephalographic delta power, typically 0.5–4.00 Hz, refers to the amplitude of low-frequency brain waves predominantly observed during NREM sleep and is widely used as a quantitative indicator for assessing sleep depth and quality.[23] Higher delta power indicates that the brain remains in the deep sleep stage for a longer duration. When sleep is insufficient, delta power markedly increases during the subsequent

Open Access Article. Published on 19 November 2025. Downloaded on 3/31/2026 6:45:20 AM.
This article is licensed under a Creative Commons Attribution 3.0 Unported Licence.

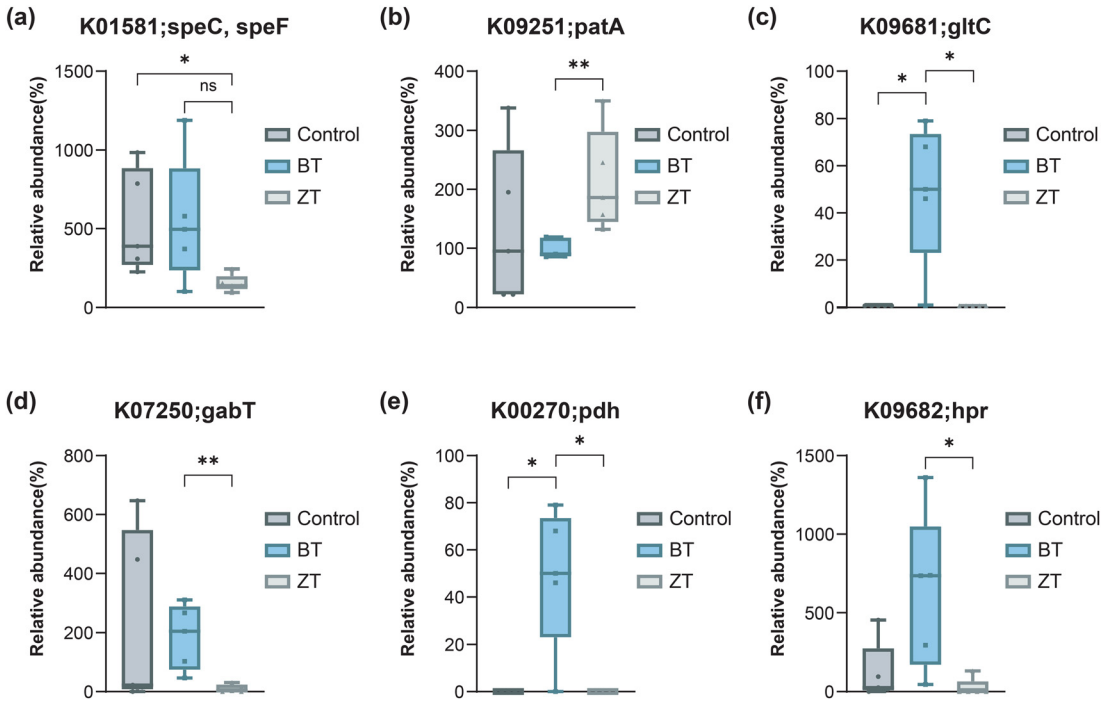

Fig. 12 Relative abundance of functional genes associated with neurotransmitter-related pathways. (a) K01581 (*speC*, *speF*), (b) K09251 (*patA*), (c) K09681 (*gltC*), (d) K07250 (*gabT*), (e) K00270 (*pdh*), and (f) K09682 (*hpr*). Data represents the relative gene abundance in CON, BT, and ZT groups. Significant differences between groups are indicated as *$p < 0.05$, **$p < 0.01$, ***$p < 0.001$ (Mann–Whitney *U* test). *Note*: CON, control group; BT, *Bacillus coagulans* IDCC 1201-treated group; ZT, zolpidem-treated group.

sleep period—a phenomenon known as delta rebound—which represents a physiological response aimed at compensating for the loss of deep sleep.[24] Thus, delta power can be regarded as an indicator of both sleep depth and restorative capacity, closely related to sleep homeostasis. However, BZD hypnotics, including diazepam and ZPD, reportedly reduce sleep quality based on EEG findings.[25] Similarly, ZPD induced a significant decline in delta power over time, which was consistent with the development of tolerance and compromised sleep quality.[26] In this preclinical context, *B. coagulans* IDCC 1201 appeared well tolerated and preserved EEG integrity; nevertheless, comprehensive safety must be established through dedicated toxicology investigations and clinical adverse-event monitoring.

Long-term EEG/EMG analysis revealed that *B. coagulans* IDCC 1201 progressively improved sleep parameters without inducing tolerance or WD effects. It enhanced sleep continuity by reducing wakefulness duration, increasing the frequency of NREMS episodes, and promoting stable transitions between NREMS and wakefulness. These results suggest that *B. coagulans* IDCC 1201 is suitable for long-term administration with sustained sleep-promoting effects, indicating its potential therapeutic application in patients with sleep disorders who are unsuitable for conventional hypnotic treatments. For instance, the use of conventional hypnotics in older patients is often limited owing to risks, such as cognitive impairment and an increased incidence of falls. However, *B. coagulans* IDCC 1201, which does not carry these risks, may be a safer and more accessible alternative.[27] Withdrawal assessment in the positive-drug arm was restricted to 48 hours after discontinuation and to EEG/EMG-derived sleep metrics; extended washout periods and standardized behavioral testing will be required to fully characterize potential withdrawal or rebound phenomena.

Fecal metabolomic analysis indicated that *B. coagulans* IDCC 1201 administration induced systemic metabolic shifts consistent with sleep-promoting mechanisms. The downregulation of TCA cycle intermediates and excitatory amino acids observed in fecal samples likely reflects alterations in gut microbial metabolism—given that these metabolites are primarily products of bacterial central carbon metabolism—rather than a direct measure of host mitochondrial activity. Such microbial shifts may still contribute to changes in energy balance within the intestinal ecosystem, which could influence host physiological states relevant to sleep regulation.[28,29] In parallel, the elevation of metabolites associated with serotonergic and dopaminergic pathways—such as 5-hydroxyindole-3-acetic acid (5-HIAA; a principal serotonin metabolite) and 4-hydroxyphenylacetic acid (4-HPAA; a gut–microbiota-derived product of tyrosine metabolism)—together with a shift toward α-tocopherol derivatives, implies enhanced mood regulation and antioxidative capacity.[30–33] Collectively, these metabolic changes support a mechanistic link between probiotic intake, modulation of energy and neurotransmitter pathways, and improved sleep physiology, emphasizing the role of the gut–brain axis in behavioral regulation.

 This journal is © The Royal Society of Chemistry 2025

Open Access Article. Published on 19 November 2025. Downloaded on 3/31/2026 6:45:20 AM.
This article is licensed under a Creative Commons Attribution 3.0 Unported Licence.

Microbiome analysis was conducted to evaluate changes in the microbial communities, including diversity metrics, taxonomic composition, and functional gene prediction. The *B. coagulans* group showed increased taxonomic richness while maintaining overall evenness and compositional similarity to vehicle, consistent with modulation of the gut microbial community. By contrast, the ZPD group exhibited features of dysbiosis, including reduced evenness. These patterns support a microbiome-based explanation for the physiological differences observed between groups. At the species level, the *B. coagulans* group was enriched for taxa implicated in the gut–brain axis and immunoregulation (*e.g.*, *B. coagulans*, *L. murinus*, *C. Arthromitus*). *B. coagulans* is a spore-forming probiotic with strong resistance to gastric acid and bile and reportedly improves gut health and mood in patients with irritable bowel syndrome.[34] *L. murinus* is a commensal bacterium known for its immunomodulatory and neuroinflammation-suppressing properties and reportedly enhances stress resilience in mouse models.[35,36] *C.* Arthromitus, a segmented filamentous bacterium, induces Th17 cell differentiation, thereby enhancing mucosal immunity and indirectly contributing to neuroimmune regulation.[37,38] These taxonomic changes were confirmed by Random Forest analysis, suggesting that *B. coagulans* IDCC 1201 contributes to the formation of a neuroprotective gut microbial ecosystem. PICRUSt2-based functional profiling suggested group-specific differences in microbial neurotransmitter-related pathways. In the ZPD group, the predicted gene abundance for ornithine decarboxylase (*speC*/*speF*; EC 4.1.1.17) and 4-aminobutyrate aminotransferase (*gabT*; EC 2.6.1.19/2.6.1.22; GABA shunt) was lower, whereas that for putrescine transaminase (*patA*; EC 2.6.1.82) was higher. The resulting putrescine is converted into GABA by *patA* and *patD*.[39,40] By contrast, the *B. coagulans* IDCC 1201 group showed higher predicted representation of *gltC* (glutamate-operon regulation) and functions linked to phenylalanine dehydrogenase (*pdh*; EC 1.4.1.20) and redox control (*hpr*; MarR family).[41] Furthermore, *hpr* has been involved in microbial oxidative-stress resistance and stabilization of the gut environment.[42–44] These findings suggest that *B. coagulans* IDCC 1201 may modulate neurotransmitter-related pathways along the microbiota–gut–brain axis, supporting its association with improvements in sleep quality. Alterations in the gut microbiome, including probiotic supplementation, can affect the brain and modulate sleep. Santi *et al.* demonstrated that sleep regulation can occur through mechanisms such as stress responses, inflammation, and neurotransmitter production.[45] These findings suggest that *B. coagulans* IDCC 1201 reorganizes sleep architecture toward a more consolidated and restorative pattern, likely mediated through modulation of the gut–brain axis and GABAergic signaling. This study contributes to the growing body of literature exploring the microbiota–gut–brain axis as a therapeutic target for regulating neurobehavioral functions. While previous studies have reported sleep modulation by certain *Lactobacillus* and *Bifidobacterium* strains, sustained improvements in both sleep quantity and quality without tolerance remain rare.[46] The dual advantages of *B. coagulans* IDCC 1201—high GABA production and host resilience—significantly enhance its translational applicability.

This study demonstrated the promising sleep-promoting effects of *B. coagulans* IDCC 1201 in animal models. However, validation in human populations is needed. *B. coagulans* IDCC 1201 is a spore-forming probiotic strain with well-established safety, and it has been consumed by humans over extended periods without reported adverse effects. Given this safety profile, along with the preclinical findings of the present study, clinical trials should confirm its efficacy in improving sleep in individuals with insomnia or stress-related sleep disturbances. The physiological, microbiota, and sleep architecture differences between rodents and humans further highlight the importance of such clinical investigations. Well-designed randomized controlled trials incorporating polysomnography and biomarker analyses will be critical to establish clinical relevance.

Further, individuals with chronic insomnia or stress-related sleep disorders often experience heightened physiological arousal, dysregulated hypothalamic–pituitary–adrenal axis activity, and alterations in gut microbiota composition, all of which can exacerbate sleep difficulties.[47,48] The ability of *B. coagulans* IDCC 1201 to enhance GABAergic signaling, stabilize sleep architecture without tolerance, and promote a neuroprotective gut microbial profile suggests a promising role as a non-sedative, microbiome-based intervention for these populations. Such properties may be particularly valuable for patients who are unsuitable for conventional hypnotics due to safety concerns or comorbidities.

This study was based on preclinical models, and a limitation is the lack of molecular level validation of mechanisms in host brain tissues. In addition, we did not measure CNS neurotransmitter levels (brain/cerebral spinal fluid). In forthcoming clinical work, we will assess circulating blood GABA concentrations as a feasible translational biomarker and interpret them alongside sleep outcomes. Moreover, this study was conducted in rodent models, which differ from humans in terms of sleep architecture, neurophysiology, and gut microbiome composition. Furthermore, behavioral assessments such as activity monitoring or anxiety-like behavior tests were not performed. Future studies incorporating these measures, alongside polysomnography in human subjects, will be important for validating the translational relevance of our findings. To clarify how *B. coagulans* IDCC 1201 influences neural circuits involved in sleep regulation, future studies should employ electrophysiological techniques such as patch clamp analysis to directly assess the effects on the activity of sleep-related neurons and GABA receptor function. Furthermore, investigations of potential interactions between *B. coagulans* IDCC 1201 and conventional hypnotics or anxiolytics could provide valuable insights for developing combinatorial therapeutic strategies.

Conclusion

This study highlights *Bacillus coagulans* IDCC 1201 as a promising probiotic candidate for sleep enhancement, com-

Open Access Article. Published on 19 November 2025. Downloaded on 3/31/2026 6:45:20 AM.
This article is licensed under a Creative Commons Attribution 3.0 Unported Licence.

bining high GABA production and gastrointestinal resilience to support its role as a natural sleep aid. *In vivo* assessments showed reduced sleep latency and improved NREMS duration and continuity without tolerance or adverse effects. The sleep-promoting effects were mediated *via* GABA-A receptor modulation at the BZD site, with preservation of delta activity indicative of sleep quality. These findings highlight the potential of *B. coagulans* IDCC 1201 as a safe, effective, and sustainable probiotic for improving sleep.

Author contributions

Hayoung Kim: conceptualization, investigation, resources, data curation, writing – original draft, visualization, project administration. Duhyeon Kim: methodology, investigation, data curation, writing – review & editing. Dong Young Lee: investigation, data curation. Won Yeong Bang: investigation, writing – original draft. Hyun Min Park: conceptualization. Han Bin Lee: writing – review & editing. Eun Ju Yun: methodology, writing – review & editing. Suengmok Cho: methodology, writing – review & editing, supervision. Jin Seok Moon: conceptualization, writing – review & editing, supervision, project administration. All authors agreed to their individual contributions. All authors read and approved the final manuscript.

Conflicts of interest

Hayoung Kim, Won Yeong Bang, Hyun Min Park, Han Bin Lee, and Jin Seok Moon are employees of Ildong Bioscience Co., Ltd. The authors declare that they have no other competing financial interests or personal relationships that could have appeared to influence the work reported in this paper.

Data availability

The study's supporting data can be found in the main manuscript.

The supplementary information file contains detailed methodology supporting the main findings of the study. See DOI: https://doi.org/10.1039/d5fo02926k.

For access to the raw data, please reach out to the corresponding author with a reasonable request.

Acknowledgements

This research was funded by Ildong Bioscience Co., Ltd. We also appreciate the constructive comments of anonymous reviewers, who improved the clarity of this manuscript.

References

1 A. C. Ouwehand, S. Salminen and E. Isolauri, Probiotics: an overview of beneficial effects, in *Lactic Acid Bacteria: Genetics, Metabolism and Applications*, ed. W. M. de Vos, A. Bruggeman and E. E. Vaughan, Springer, Dordrecht, 2002, pp. 279–289.
2 A. Żarowska, From probiotics to psychobiotics – the gut-brain axis in psychiatric disorders, *Benefic. Microbes*, 2020, **11**, 717–732.
3 J. Woo, H. Lim, H. S. Lee, M. B. Park, S. Kim and H. J. Kim, 3-Carene, a phytoncide from pine tree has a sleep-enhancing effect by targeting the GABAA-benzodiazepine receptors, *Exp. Neurobiol.*, 2019, **28**, 593.
4 N. Zhao, T. Yu and F. Yan, Probiotic role and application of thermophilic *Bacillus* as novel food materials, *Trends Food Sci. Technol.*, 2023, **138**, 1–15.
5 Y. Liu, Y. Yu, S. Lu, K. Tan, P. Jiang, P. Liu and Q. Peng, Impact of probiotics on sleep quality and mood states in patients with insomnia: a systematic review and meta-analysis, *Front. Microbiol.*, 2025, **16**, 1596990.
6 R. R. Gilley, The role of sleep in cognitive function: the value of a good night's rest, *Clin. EEG Neurosci.*, 2023, **54**, 12–20.
7 A. R. Ramos, A. G. Wheaton and D. A. Johnson, Peer reviewed: sleep deprivation, sleep disorders, and chronic disease, *Prev. Chronic Dis.*, 2023, 20, DOI: 10.5888/pcd20.220236.
8 N. L. Harrison, Mechanisms of sleep induction by GABA, *J. Clin. Psychiatry*, 2007, **68**, 6–12.
9 J. Cabaj, J. Bargieł and E. Soroka, Benzodiazepines and z-drugs – between treatment effectiveness and the risk of addiction, *J. Educ., Health Sport*, 2023, **46**, 468–480.
10 M. Y. Um, M. Y. Kim, S. H. Hwang, Y. J. Ahn, M. H. Kim, M. S. Ha and M. Y. Jung, Curcuminoids, a major turmeric component, have a sleep-enhancing effect by targeting the histamine H1 receptor, *Food Funct.*, 2022, **13**, 12697–12706.
11 H. J. Han, H. J. Lee and J. W. Choi, Sleep-time variation for ethanol and the hypnotic drugs tribromoethanol, urethane, pentobarbital, and propofol within outbred ICR mice, *Biol. Pharm. Bull.*, 2003, **26**(6), 825–829.
12 P. Franken, A. Malafosse and M. Tafti, Genetic variation in EEG activity during sleep in inbred mice, *Am. J. Physiol.: Regul., Integr. Comp. Physiol.*, 1999, **275**(4), R1127–R1137.
13 V. K. Shah, J. H. Choi, J. Y. Han, M. K. Lee and J. T. Hong, Pachymic acid enhances pentobarbital-induced sleeping behaviors through the GABA_A-ergic system in mice, *Biomol. Ther.*, 2014, **22**(4), 314–320.
14 Y. O. Kwon, S. H. Hong, J. H. Kim and J. A. Kim, Rosmarinic acid potentiates pentobarbital-induced sleep behaviors in mice, *Biomol. Ther.*, 2016, **24**(4), 450–456.
15 L. De Gennaro and M. Ferrara, Sleep spindles: an overview, *Sleep Med. Rev.*, 2003, **7**, 423–440.
16 M. Ye, H. Kim, Y. Jang, J. H. Lee, Y. C. Jung, Y. H. Kim and Y. C. Ryu, GABALAGEN facilitates pentobarbital-induced

 This journal is © The Royal Society of Chemistry 2025

Open Access Article. Published on 19 November 2025. Downloaded on 3/31/2026 6:45:20 AM.
This article is licensed under a Creative Commons Attribution 3.0 Unported Licence.

sleep by modulating the serotonergic system in rats, *Curr. Issues Mol. Biol.*, 2024, **46**, 11176–11189.

17 W. Gao, S. Wu, L. Chen, Q. Liu, Y. Chen and L. Liu, Effects of *Bacillus coagulans* TBC169 on gut microbiota and metabolites in gynecological laparoscopy patients, *Front. Microbiol.*, 2024, **15**, 1284402.

18 J. Brandt and C. Leong, Benzodiazepines and Z-drugs: an updated review of major adverse outcomes reported on in epidemiologic research, *Drugs R&D*, 2017, **17**, 493–507.

19 M. Kayabekir, in *Sleep Medicine and the Evolution of Contemporary Sleep Pharmacotherapy*, IntechOpen, London, 2021, ch. 1, pp. 1–18.

20 R. E. Brown, Y. Basheer, J. T. McKenna, R. E. Strecker and R. W. McCarley, Control of sleep and wakefulness, *Physiol. Rev.*, 2012, **92**, 1087–1187.

21 K.-S. Park, M.-B. Park, Y.-R. Kim, S.-H. Kim and H.-J. Kim, (−)-Epigallocatechin-3-O-Gallate augments pentobarbital-induced sleeping behaviors through Cl^- channel activation, *J. Med. Food*, 2011, **14**, 1456–1462.

22 S. Zhu, L. Noviello, W. Teng, D. Walsh, J. Kim, E. Shen, M. Laprairie, J. T. Yip and R. L. Macdonald, Structural and dynamic mechanisms of GABAA receptor modulators with opposing activities, *Nat. Commun.*, 2022, **13**, 4582.

23 J. Lee, S. Park, M. Kim, H. Lim, H. J. Kim and Y. Lee, Multitask exercise increases delta power in non-rapid eye movement sleep among older female adults: a randomized crossover trial, *NeuroImage*, 2025, **310**, 121105.

24 I. Feinberg and I. G. Campbell, Total sleep deprivation in the rat transiently abolishes the delta amplitude response to darkness: implications for the mechanism of the "negative delta rebound", *J. Neurophysiol.*, 1993, **70**(6), 2695–2699.

25 I. Feinberg, T. Maloney and I. G. Campbell, Effects of hypnotics on the sleep EEG of healthy young adults: new data and psychopharmacologic implications, *J. Psychiatr. Res.*, 2000, **34**, 423–438.

26 K. A. Wafford and B. Ebert, Emerging anti-insomnia drugs: tackling sleeplessness and the quality of wake time, *Nat. Rev. Drug Discovery*, 2008, **7**, 530–540.

27 J. L. Schroeck, J. T. Ford, A. L. Conway, L. H. Kurtzhalts, T. L. Gee, B. S. Vollmer and S. S. Mergenhagen, Review of safety and efficacy of sleep medicines in older adults, *Clin. Ther.*, 2016, **38**, 2340–2372.

28 M. Dworak, T. W. McCarley, R. P. Kim, J. Basheer and R. W. Strecker, Sleep and brain energy levels: ATP changes during sleep, *J. Neurosci.*, 2010, **30**, 9007–9016.

29 N. Goldstein-Daruech, J. E. Hallworth, J. R. Winer and R. D. Shores, Effects of excitatory amino acid antagonists on the activity of inferior colliculus neurons during sleep and wakefulness, *Hear. Res.*, 2002, **168**, 174–180.

30 J. M. Monti and H. Jantos, The roles of dopamine and serotonin, and of their receptors, in regulating sleep and waking, *Prog. Brain Res.*, 2008, **172**, 625–646.

31 J. R. Lenchner and C. Santos, *Biochemistry, 5-Hydroxyindoleacetic Acid*, StatPearls, StatPearls Publishing, Treasure Island (FL), 2023.

32 L. Armand, M. Andriamihaja, S. Gellenoncourt, V. Bitane, A. Lan and F. Blachier, In vitro impact of amino acid-derived bacterial metabolites on colonocyte mitochondrial activity, oxidative stress response and DNA integrity, *Biochim. Biophys. Acta, Gen. Subj.*, 2019, **1863**, 1292–1301.

33 E. Reiter, Q. Jiang and S. Christen, Anti-inflammatory properties of α- and γ-tocopherol, *Mol. Aspects Med.*, 2007, **28**, 668–691.

34 M. Majeed, K. Nagabhushanam, S. Arumugam, M. Khetarpal and M. Majeed, *Bacillus coagulans* MTCC 5856 for the management of major depression with irritable bowel syndrome: a randomised, double-blind, placebo controlled, multi-centre, pilot clinical study, *Food Nutr. Res.*, 2018, **62**, DOI: 10.29219/fnr.v62.1218.

35 H.-X. Fan, X. Wang, Y. Li, J. Li, X. Wang, L. Feng and W. Qiu, Heat-killed Lactobacillus murinus confers neuroprotection against dopamine neuronal loss by targeting NLRP3 inflammasome, *Bioeng. Transl. Med.*, 2023, **8**, e10455.

36 A. R. Merchak, A. L. Hinkle, N. B. Savidge, K. G. O'Mahony, D. M. Lyte, C. A. Lowry and J. F. Cryan, Lactobacillus from the Altered Schaedler Flora maintain IFNγ homeostasis to promote behavioral stress resilience, *Brain, Behav., Immun.*, 2024, **115**, 458–469.

37 H. L. Klaasen, C. A. van der Heijden, J. F. M. M. van den Brink and W. M. A. de Vos, Apathogenic, intestinal, segmented, filamentous bacteria stimulate the mucosal immune system of mice, *Infect. Immun.*, 1993, **61**, 303–306.

38 E. Lécuyer, A. Rakotobe, S. Lengliné-Garnier, N. Lebreton, E. Picard, V. Juste, J. F. Cerf-Bensussan and N. Gaboriau-Routhiau, Segmented filamentous bacterium uses secondary and tertiary lymphoid tissues to induce gut IgA and specific T helper 17 cell responses, *Immunity*, 2014, **40**, 608–620.

39 B. L. Schneider, V. J. Hernandez and L. Reitzer, Putrescine catabolism is a metabolic response to several stresses in Escherichia coli, *Mol. Microbiol.*, 2013, **88**, 537–550.

40 J. M. P. Jorge, C. Leggewie and V. F. Wendisch, A new metabolic route for the production of gamma-aminobutyric acid by Corynebacterium glutamicum from glucose, *Amino Acids*, 2016, **48**, 2519–2531.

41 B. J. Shelp, A. W. Bown and M. D. McLean, Metabolism and functions of gamma-aminobutyric acid, *Trends Plant Sci.*, 1999, **4**, 446–452.

42 S. P. Cohen, H. Hächler and S. B. Levy, Genetic and functional analysis of the multiple antibiotic resistance (mar) locus in Escherichia coli, *J. Bacteriol.*, 1993, **175**, 1484–1492.

43 D. W. Ellison and V. L. Miller, Regulation of virulence by members of the MarR/SlyA family, *Curr. Opin. Microbiol.*, 2006, **9**, 153–159.

44 J. A. Alves, M. S. G. Oliveira, R. B. Bezerra, E. M. Silva, A. F. Araujo, R. V. Barbosa, C. S. Barros, J. R. S. Nascimento and A. G. Souza, The MarR family regulator OsbR controls oxidative stress response, anaerobic nitrate respiration, and

Open Access Article. Published on 19 November 2025. Downloaded on 3/31/2026 6:45:20 AM.
This article is licensed under a Creative Commons Attribution 3.0 Unported Licence.

biofilm formation in Chromobacterium violaceum, *BMC Microbiol.*, 2021, **21**, 1–14.

45 D. Santi, A. Brigante, A. Neri, M. Spaggiari, V. Turrini, F. Zagni, M. Simoni and C. Rochira, Microbiota composition and probiotics supplementations on sleep quality—A systematic review and meta-analysis, *Clocks Sleep*, 2023, **5**, 770–792.

46 B. Yu, Y. Liu, H. Zhang, Y. Xu, L. Zhang and J. Liu, Effect of probiotics and paraprobiotics on patients with sleep disorders and sub-healthy sleep conditions: a meta-analysis of randomized controlled trials, *Front. Neurol.*, 2024, **15**, 1477533.

47 D. Riemann, K. Spiegelhalder, B. Feige, C. Voderholzer, U. Berger, M. Perlis, C. Nissen and R. J. Van Someren, The hyperarousal model of insomnia: a review of the concept and its evidence, *Sleep Med. Rev.*, 2010, **14**, 19–31.

48 B. Pala, L. G. Urbinati, F. M. Salvio, A. P. Isidori and M. Viceconti, Gut microbiota dysbiosis and sleep disorders: culprit in cardiovascular diseases, *J. Clin. Med.*, 2024, **13**, 3254.

 This journal is © The Royal Society of Chemistry 2025